UNIVERSITI
TEKNOLOGI
PETRONAS

Pressure Transient Analysis in Injection Wells

by

Hasnain Ali Asfak Hussain

Dissertation submitted in partial fulfilment of
the requirement for the
MSc. Petroleum Engineering

July 2012

Universiti Teknologi PETRONAS
Bandar Seri Iskandar
31750 Tronoh
Perak Darul Ridzuan

CERTIFICATE OF APPROVAL

Pressure Transient Analysis in Injection Wells

by

Hasnain Ali Asfak Hussain

A project dissertation submitted to the
Petroleum Engineering Programme
Universiti Teknologi PETRONAS
in partial fulfilment of the requirement for the
MSc. of PETROLEUM ENGINEERING

Approved by,

_____

Prof. Noaman EL - Khatib

UNIVERSITI TEKNOLOGI PETRONAS

TRONOH, PERAK

July 2012

CERTIFICATION OF ORIGINALITY

This is to certify that I am responsible for the work submitted in this project, that the original work is my own except as specified in the reference and acknowledgements, and that the original work contained herein have not been undertaken or done by unspecified sources or persons.

_____

HASNAIN ALI ASFAK HUSSAIN

ABSTRACT

A composite reservoir model is used to analyze well tests from a variety of secondary and tertiary recovery projects. Water flooding is widely used as a secondary recovery technique. Due to injection, a water bank and oil bank regions would be formed. Each region has its own rock and fluid properties. and the main scope of well test study during injection would give a clear idea of the displacement process of oil by water and to study the variation in fluid parameters in the reservoir. Pressure transient analysis of a two-region composite reservoir is considered extensively in the literature.

An infinite reservoir with injection well placed at the centre of the reservoir is used to inject water at a constant rate, this gives rise to the applicability of line source solution. 1 dimensional radial homogeneous model is developed using ECLIPSE 100. Injection and falloff analyses are made on this injection well, by initially assuming zero wellbore storage effects and zero skin.

Initial studies from the pressure transient analysis showed the effects of the two banks formed. Injection and falloff studies were carried out for the initial case first. The pressure vs. time data generated from the numerical simulation model ECLIPSE 100 for injection and falloff tests were further studied and their properties like skin, permeability and mobility were evaluated and compared with the input data. Saturation profile showed the movement of the two bank system, whereas, the total mobility profile showed variation in saturation gradient and the changes in total mobility away from the wellbore.

Further studies were made by changing few input parameters and studying pressure behavior for both injection and falloff tests. Parameters studied were, effect of changing oil viscosity, relative permeability, wellbore storage, and skin. The changes in mobility ratio by changing oil viscosity showed different pressure behavior for each case, variation in the pressure curves were clearly visible after the flood out zone was reached. Multi-bank analysis method was found to be applicable for different sets of relative permeabilities. The effect of skin factor was only observed

when pressure difference was plotted against time, and showed no effect on the semi-log plot, derivative plot and the mobility profile. Presence of wellbore storage on pressure curves was dominant during the early time region and the elimination of wellbore storage effects is very important for accurate interpretations of the early time region.

ACKNOWLEDGEMENTS

First of all I would like to express my gratitude and take immense pleasure in thanking Prof. Noaman EL – Khatib for his constant guidance and supervision throughout the project, without his knowledge and assistance this project would not have been successful. I also would like to thank all those people who has contributed in any way for the success of this Individual project. I would also like to express my gratitude to Dr. Ismail B. Mohd Saaid and Dr. Khalik B. Mohd Sabil for being very helpful in giving us assistance and advices during this project. I would also like to thank Mr. Saleem Tunio, the coordinator of this project, for support and guidance he gave to successfully commence this project.

I would like to express my sincere gratitude to UTP and Herriot Watt for providing us an opportunity to enhance my knowledge and research skills through this project.

Finally, yet importantly, I would like to express my heartfelt thanks to my beloved parents and family for their blessings and support throughout my study period, and my friends/classmates for their help and wishes for the successful completion of this project.

Table of Contents

LIST OF FIGURES

LIST OF TABLES

ABBREVIATIONS

IOR	Improved oil recovery
EOR	Enhanced Oil Recovery
BU	Buildup
DD	Drawdown

NOMENCLATURE

B : Formation volume factor, RB / STB

c : Compressibility, psi^{-1}

C : Wellbore storage coefficient, bbl/psi

f : Fractional flow

g : Acceleration due to gravity, ft/sec^2

h : Pay thickness, ft

k : Absolute permeability, md

k_r : Relative permeability

M : Mobility ratio

M : Slope

P : Pressure, psi

P_c : Capillary pressure, psi

P_{wf} : Flowing bottom-hole pressure, psi

P_{ws} : Shut-in bottom-hole pressure, psi

q : Flow rate, STB / day

r : Radial distance, ft

S : Saturation

s : Skin factor

t : Time, hour

Δt_{fx} : Intersection time, hour

Δt_{Dfx} : Dimensionless intersection time

γ : Euler's constant

Greek Symbols

Δ : Difference operator

α : Alpha

ϕ : Porosity

λ : Mobility, md / cp

μ : Viscosity, cp

θ : Thera direction

ρ : Density, lbm / ft^3

d : Derivative operator

∂ : Derivative operator

Subscripts

1 : Zone 1

2 : Zone 2

avg : Average

D : Dimensionless

e : Equivalent

f : Front, pore volume

ff : Flood front

fo : Floodout

i, inj : injection condition

m : Fluid phase (oil or water)

o : Oil

ro : Irreducible oil

t : Total

w : Water

wc : Connate water

Superscripts

$^{\|}$: Derivative operator

CHAPTER 1

INTRODUCTION

Well test analysis is a branch of reservoir engineering. Information obtained from pressure transient tests about in situ reservoir conditions is essential to determine the productive capacity of the well and the reservoir. Testing injection wells is important for operation and efficient planning of both secondary and tertiary recovery projects. Throughout the life of an injection or a production well, from exploration to abandonment, a sufficient amount of well test data are collected to describe well condition and behavior. Pressures are very useful data in reservoir engineering. Directly or indirectly, they enter into all phases of reservoir engineering calculations. In general all well test analysis is conducted to meet the following objectives:

- To evaluate well condition and reservoir characterization.
- To obtain reservoir parameters for reservoir description, which includes skin factor, permeability, average reservoir pressure, drainage area, pressure and saturation distribution in the reservoir, etc;

1.1 Background

Throughout the world numerous water flooding projects are carried out to increase oil recovery. In offshore reservoirs, especially in large oil fields, water injection is initiated during the early stages of reservoir development. In mature water flooded fields, injection wells may be as numerous as the production wells. As injection begins, a saturation gradient is established in the reservoir, forming a region of high water saturation around the wellbore. As we move away from the wellbore, water saturation decreases until the flood front is reached. Therefore, a two bank reservoir is formed, i.e, water bank and an oil bank. Ahead of the injection front an oil bank with initial water saturation is located. This would yield different fluid mobilities in each bank and the knowledge of variation of mobilities and saturation

in the reservoir is needed to conduct water flooding operations effectively in the reservoir model.

Application of injection well testing includes water flooding, pressure maintenance by water or gas injection, gas recycling, and enhanced oil recovery (EOR) operations. The objectives of injection tests are the same as those of production tests, namely permeability, skin, average reservoir pressure, detection of reservoir heterogeneity and front tracking, i.e, determination of the fluid interfaces that form in the reservoir as a result of injecting fluid that differs in its characteristics from the reservoir fluid. Injection performance (injectivity) and increasing wellbore damage over a long period of time are important to the economics of any recovery project.

Injection well testing involves application of one or more of the following methods:

1. Injectivity test
2. Pressure falloff test
3. Step-rate injectivity test

Step-rate injectivity test deals with the determination of the pressure at which fracturing could be induced in the reservoir rock. In this test the injection rate is stepped up in successive periods for a certain period of time. In this thesis we only concentrate on injectivity test and pressure falloff test.

In an injectivity test, bottom-hole pressure is recorded as soon as injection begins. If the injected fluid has exactly the same properties (density, viscosity, compressibility, and wetting characteristics) of the reservoir fluids, then an injectivity test would be similar to a pressure drawdown test except that the rate q would be negative. If the density of the injected fluid differs from the reservoir fluid, then the injected fluid will tend to ride over or sink below the reservoir fluid, this would therefore give false interpretation of the net pay, h, as compared to the drawdown tests under single phase fluid conditions. If the compressibility, wetting characteristics, and viscosity of the injected fluid are different from the reservoir fluid, an interface of front will form in the reservoir between reservoir and injected fluid, the permeability of the reservoir rock to each fluid will depend on its saturation, i.e relative permeability will play an important role.

Usually falloff test is done after pressure injectivity test. During a falloff test, injection is stopped and pressure is recorded at each time interval. Therefore pressure falloff test is similar to a pressure buildup test, only if the properties of reservoir fluid match with that of injected fluid. On the other hand, if the injected fluid has filled a substantial area around the well and the properties of the reservoir fluid differs with that of injected fluid, then a falloff test or a two-rate falloff test which is preceded by an injection period of a short duration could be interpreted in exactly the same way as a buildup or as a two-rate test. In this case the pressure transients would have travelled only a short distance away from the well, hence a falloff test preceded by a short injection period would not be affected by the fluid interface in the reservoir between injected and reservoir fluid and therefore cannot be used for front tracking. If the area occupied by the injected fluid is quite large then the information obtained from an injection test could be comparable with that of the production test.

For simplicity, this thesis will be restricted to a case of homogeneous single layered reservoir containing a single-phase fluid of constant properties. Saturation and injection pressure are also considered to be constant before injection, water is injected at a constant rate through a well which completely penetrates the formation, and the injection plot is even and independent of the density contrast between injected and reservoir fluids.

1.2 Problem Statement

Pressure transient testing for injection and falloff tests are used to estimate the reservoir properties of injection wells especially during secondary and tertiary recovery projects. The knowledge of near wellbore conditions and reservoir properties in injection wells is very important. When a fluid is injected into the reservoir, fluid banks are formed containing different fluid properties. This causes the nature of the pressure curves changing with change in each fluid property. The purpose of this project is to perform a pressure transient study on an injection well and analyze the pressure behavior of injection and falloff tests. Further studies will

also be carried out to study the pressure behavior when certain parameters like properties of the reservoir, injection fluid or reservoir fluid are changed.

1.3 Objectives

The objectives of this work are to study the pressure transient behavior of a single well during injection period and shut in period. Parameters like skin, permeability and mobility from the injection and falloff curves will be evaluated. Distance to the flood front is also to be evaluated with mobility variation throughout the reservoir is compared with the derivative curves and from saturation distribution curves obtained from eclipse. And finally a sensitivity study is conducted to understand the effects on the pressure curves when the parameters mentioned below are varied.

a) Viscosity of oil
b) Relative permeability
c) Skin
d) Wellbore Storage

1.4 Scope of Study

Well testing in general is used in industries to obtain the estimates of the reservoir properties under in-situ reservoir conditions and to determine the productive capacity of a reservoir. Along with this well testing has many other objectives which provide vital information about the reservoir. Information obtained from this is very important for the industry to predict the future of the reservoir and its recovery which could be obtained by injecting fluids in the reservoir, this allows the industry to consider its options and if necessary use other alternatives to improve recovery. Injection well testing also provides information about the in-situ fluid properties and the changes they occur due to injection of fluids, these data are vital when EOR or IOR considerations are to be taken in the future. Injection well testing

in short plays an important role in a petroleum industry, and all the data mentioned above, are mainly obtained by analyzing the pressure behavior of the reservoir and the well.

CHAPTER 2

THEORY AND LITERATURE REVIEW

2.1 Line Source Solution

Line source solution is applicable only for infinite acting reservoirs and assumes that the wellbore radius is very small when compared to the reservoir radius. Pressure calculation at any point in the reservoir using flow rate at the well can be achieved by using the line source approximation. The concept of superposition also can be used to determine the effect of any boundaries or barriers by studying the effect of pressure distribution from more than one well, provided the reservoir is still infinite acting.

$$P_i - P(r,t) = -\frac{q\mu}{4\pi kh}\left[Ei\left(-\frac{\emptyset\mu c_t r^2}{4kt}\right)\right] \quad \text{Eq (2.1)}$$

Where, Ei(-y) is the exponential integral of y, which is expressed as

$$Ei(-y) = -\int_y^{\infty} \frac{e^{-y}}{y} dy \quad \text{Eq (2.2)}$$

Very shortly when production starts, i.e when y<0.01 the line source solution can be approximated by replacing the exponential integral term with a simple logarithm function [**1**].

$$P_{wf} = P_i - \frac{q\mu}{4\pi kh}\left(\frac{\ln 4kt}{\gamma\emptyset\mu c_t r_w^2}\right) \quad \text{Eq (2.3)}$$

2.2 Diffusivity Equation

All pressure analysis techniques are derived from solutions to the partial differential equations that describe the flow of fluids through porous media, utilizing

various initial and boundary conditions. This mathematical description of fluid flow is based on three physical principles: (1) the law of conservation of mass, (2) Darcy's law, and (3) equations of state. Partial differential equation in a porous medium for a single-phase fluid is given as follows:

$$\frac{\partial}{\partial x}\left(\frac{k\rho}{\mu}\frac{\partial P}{\partial x}\right) = \emptyset c_t \rho \frac{\partial P}{\partial t} \qquad \text{Eq (2.4)}$$

The above equation is non linear because of pressure dependent terms such as compressibility, viscosity, and density. Linearising the above equation by eliminating density term and assuming compressibility is small and constant, gives raise to liner diffusivity equation which is simply the relation between pressure gradient and the change in pressure with time, and is expressed as follows:

$$\frac{\partial^2 P}{\partial x^2} = \left(\frac{\emptyset \mu c_t}{k}\right)\frac{\partial p}{\partial t} \qquad \text{Eq (2.5)}$$

Where, $\frac{k}{\emptyset \mu c_t}$ is the diffusivity constant.

For a radial model where flow occurs parallel to the XY planes within a layer of constant height h, and making assumptions same as in the case of linear flow, gives raise to the radial diffusivity equation [**1**]

$$\frac{1}{r}\frac{\partial}{\partial r}\left(r\frac{\partial P}{\partial r}\right) = \frac{\emptyset \mu c_t}{k}\frac{\partial P}{\partial t} \qquad \text{Eq (2.6)}$$

2.3 Conventional Well Testing

Conventional well testing for measuring pressure in the wells started way back in 1920's. Drill stem test (DST) was first introduced for testing exploration or appraisal wells for open hole conditions and then as technology improved DST was used after the borehole was cased, cemented and perforated. In a typical well test a small drawdown is created by producing a well at a known flow rate and then shut-in by opening and closing a testing valve, bottom hole pressure is also simultaneously

recorded by the transducer [**2**]. Drawdown tests are primarily designed to characterize reservoir flow which includes the evaluation of skin, permeability, reservoir boundaries, drainage area, productivity of the well etc [**3**].

Pressure buildup tests are conducted when a well, after producing for sometime is shut-in, as a result of completely shutting the well, the bottom hole pressure thus builds up with time. Pressure buildup analysis is used to evaluate and estimate properties of the reservoir, which includes, permeability, skin, average drainage area, reservoir pressure etc. Buildup tests are usually analyzed using Horner plot, which is a plot of build up pressure against Horner time function [**3**].

$$\frac{\ln(t_p + \Delta t)}{\Delta t} \qquad \text{Eq (2.7)}$$

Injection well testing has its applications as discussed in Chapter 1. Injection well test is a mirror image of pressure drawdown test, but for a unit mobility ratio injection and drawdown tests would be identical except that the constant injection rate q_{inj} would be negative. Injection well tests have its objectives similar to those of production tests, namely the estimation of permeability, skin, average reservoir pressure, reservoir heterogeneity and front tracking. The equations used to determine these properties are mentioned below:

$$P_{wf} = P_{1\,hour} + mlog(t) \qquad \text{Eq (2.8)}$$

The above equation shows the relationship between bottom hole pressure and logarithm of injection time, when plotted would show a straight line with a slope m and intercept of the bottom hole pressure after 1 hour of injection time. Slope m is defined as:

$$m = \frac{162.6 q_{inj} B \mu}{kh} \qquad \text{Eq (2.9)}$$

A log-log plot of (P_{wf} - P_i) vs. injection time can be used effectively to estimate the duration of the wellbore storage effects by using the following equation:

$$t > \frac{(200{,}000 + 12{,}000s)C}{\frac{kh}{\mu}} \qquad \text{Eq (2.10)}$$

Where, t is time that points out the end of wellbore storage effects.

Once the semi log straight line is plotted the permeability, thickness product and skin factor can be estimated using the following equations:

$$kh = \frac{162.6 q_{inj} B \mu}{m} \qquad \text{Eq (2.11)}$$

$$s = 1.151\left[\frac{P_{1hr} - P_i}{m} - log\left(\frac{k}{\emptyset \mu C_t r_w^2}\right) + 3.23\right] \qquad \text{Eq (2.12)}$$

The well is shut-in and falloff test is conducted once the injectivity test is completed for a total injection time of t_p at a constant injection rate q_{inj}. Pressure is recorded from the moment the well is shut-in and the recorded pressure is analyzed using Horner plot

$$P_{wf} = P^* + mlog\left(\frac{t_p + \Delta t}{\Delta t}\right) \qquad \text{Eq (2.13)}$$

Where P^* is initial reservoir pressure in a new field

The skin factor is estimated using the following equation, and the slope and the permeability, thickness product equations are the same as mentioned above [**4**]. Figure 1 shows an ideal pressure and rate response with time for injection and falloff periods.

$$s = 1.151\left[\frac{P_{wf\ at\ \Delta t=0} - P_{1hr}}{m} - log\left(\frac{k}{\emptyset \mu C_t r_w^2}\right) + 3.23\right] \qquad \text{Eq (2.14)}$$

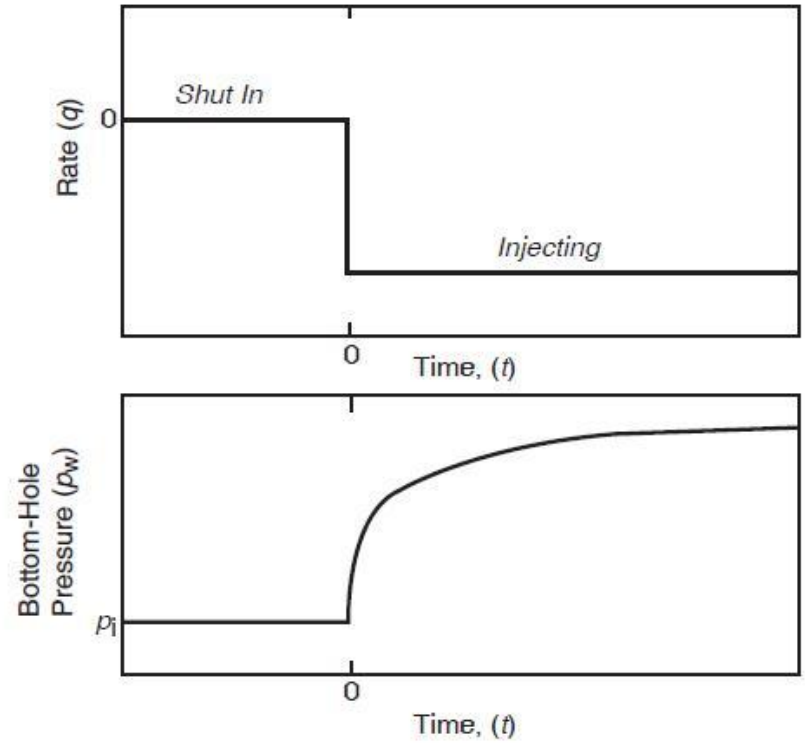

Figure 1: Rate and pressure response for shut-in and injection periods [**5**]**.**

2.4 Composite Reservoir

A composite reservoir is made up of two or more regions. Each region has its own rock and fluid properties. A composite system can occur naturally or artificially created. Oil and water regions or oil and gas regions or aquifers with two different permeabilities forming two regions are few examples of naturally occurring two region composite systems. Water flooding, steam injection, gas injection, polymer flooding and other secondary and tertiary recovery projects are examples of artificially created two region composite systems.

Hazebroek, et al. in 1985 [**6**] analyzed pressure falloff data from water injection wells assuming two different cases; Case 1 where water and oil are assumed to have same properties, and Case 2 where water and oil bank properties are different. Yeh and Agarwal in 1989 [**7**] analyzed pressure transient analysis of injection wells in reservoirs with multiple fluid banks to calculate mobility profile in the reservoir and fluid bank radii. It was assumed that the injection well was located at the centre of

the cylindrical reservoir. Well penetrating the entire pay thickness and water was injected at a constant rate. Reservoir was assumed to be homogenous filled with oil and water, and constant initial reservoir pressure and initial water saturation everywhere in the reservoir before injection. Outer boundary was maintained at a constant pressure equal to the initial reservoir pressure.

Ambastha in 1988 [**8**] presented, guidelines for the applicability of different methods to estimate front radius. In a region near the front, dynamic phenomena such as phase changes and multi phase flow effects could cause a sharp pressure drop at the front. Such a sharp pressure drop was modeled as a thin skin at the front in his study using Laplace transformation, this effect of skin at the front is similar to the effects of storativity ratio and would yield large errors in parameter estimation using type curve matching method if the thin skin was neglected. Pressure derivative of a three region composite reservoir was also discussed. And finally he established the applicability and the limitations of the deviation time method to estimate front radius of composite reservoirs from several well tests.

Figure 2 shows a schematic diagram of a two-region, radial composite reservoir. Inner and outer regions of the composite reservoir have uniform but different rock and fluid properties separated by discontinuity. ‘R’ is the front radius which is an important parameter in composite reservoirs.

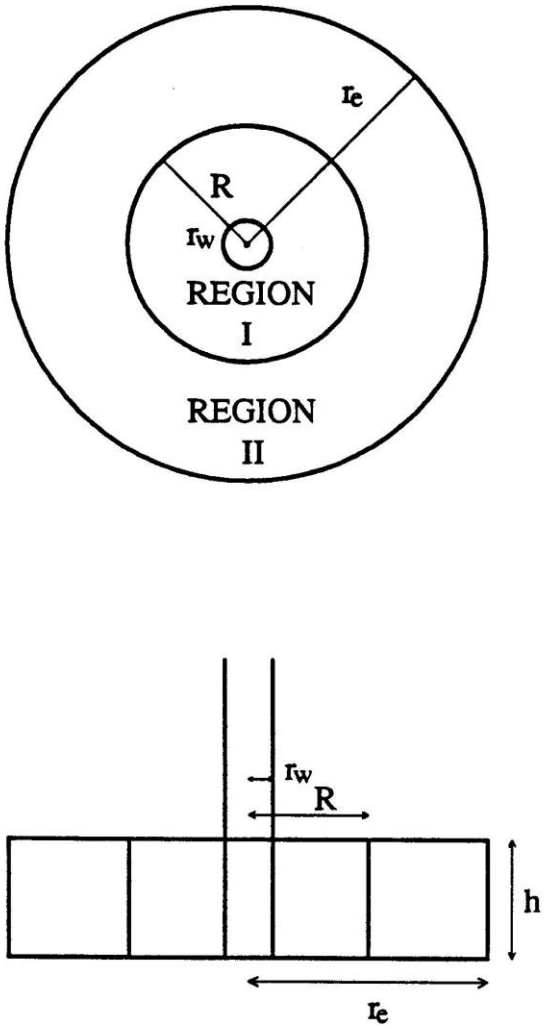

Figure 2: Two region, radial composite reservoir [**8**]

Saturation profile and displacement model from Buckley-Leverett has a major role to play in the injection well testing models discussed in this thesis. Buckley and Leverett [**9**] published a paper in 1942 and is called as frontal displacement theory, which describes the mechanism by which displacement is effected and the advantages of water over gas as a displacing agent.

Leverett [**10**] in 1941 had analyzed the concept of fractional flow and developed equations to estimate the performance of water flooding. Leverett's general formula for fractional flow:

$$f_w = \frac{1 + \frac{k_o A}{q_t \mu_o}\left(\frac{dP_c}{dx} - g\Delta\rho sin\alpha\right)}{1 + \frac{\mu_w}{\mu_o}\frac{k_o}{k_w}} \qquad \text{Eq (2.15)}$$

Where $\boldsymbol{f}_w$ is the fractional flow, q_t is the total flow rate or injection rate (bbl/day), A is the cross-sectional area (ft^2), $\frac{\partial P_C}{\partial x}$ is the capillary pressure gradient, g is the gravitational constant, Δρ is density difference between water and oil (ρ_w - ρ_o) (g/cm^3), α is the reservoir inclination angle, k_o and k_w are effective permeability for oil and water respectively (md), $\mu_o$and $\mu_w$are viscosity of oil and water respectively (cp). When the dip angle (α = 0) the reservoir is horizontal and neglecting the capillary pressure term, Leverett came out with a simplified equation for the fractional curve:

$$f_w = \frac{1}{1 + \frac{\mu_w}{\mu_o}\frac{k_{ro}}{k_{rw}}} \qquad \text{Eq (2.16)}$$

Figure 3 shows the fractional flow curve vs water saturation:

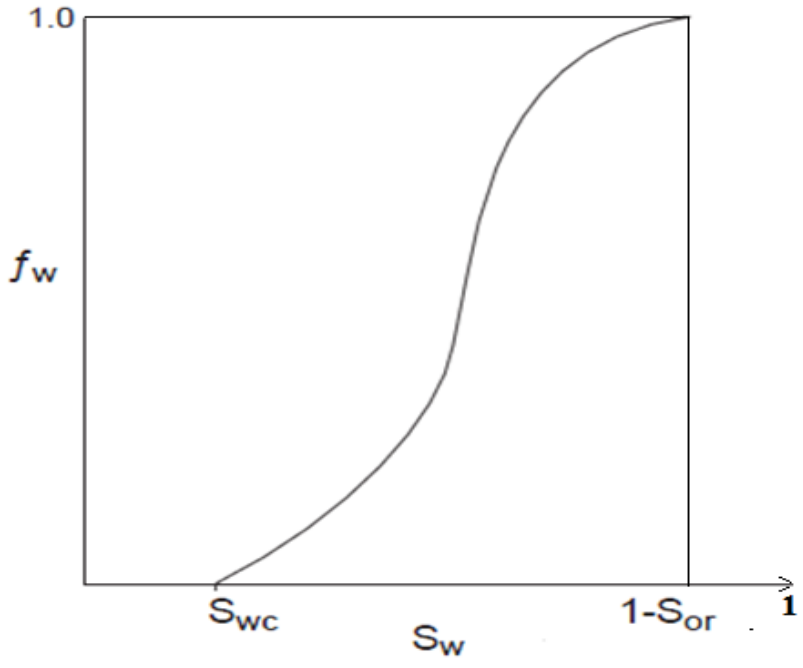

Figure 3: Fractional flow vs. water saturation [10].

Buckley and Leverett [**9**] presented the basic equation for describing two-phase, immiscible displacement in a liner system. Using material balance for the displacing fluid they developed an equation which suggests the position of water saturation S_w.

$$(x)_{sw} = \frac{5.615 i_w t}{\emptyset A}\left(\frac{df_w}{dS_w}\right)_{swf} \qquad \text{Eq (2.17)}$$

Where $(x)_{sw}$ is the distance from the injection well at any given saturation S_w, i_w is the water injection rate in bbl/day, t is time in days, $(df_w/dS_w)_{swf}$ is obtained graphically by drawing a tangent to the f_w curve.

Figure 4 shows the saturation profile in accordance with Buckley-Leverett model as discussed previously which develops in the reservoir as a result of injecting water into an oil bearing zone. PVT and representative relative permeability data are generally required to obtain the saturation profile. Figure 5 shows a plan view of the saturation distribution in the vicinity of the injection well and three distinctive zones, flood out zone, transition zone, and uninvaded zone can be seen. The flood out zone i.e water bank is adjacent to the injection well with residual oil saturation. Invaded zone contains oil saturation that varies between S_{or} and the initial oil saturation, S_{oi}. A sudden change in saturation is observed at the beginning of the uninvaded zone, which is known as the flood front which contains initial water saturation, S_{wi}. The initial water saturation can either be greater or equal to the irreducible water saturation, S_{wc}.

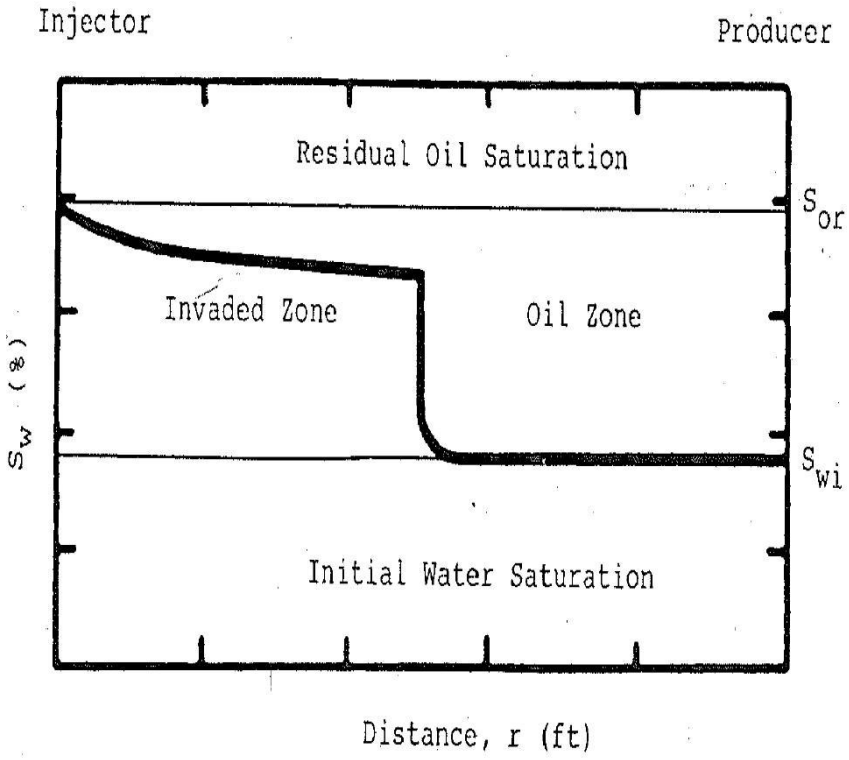

Figure 4: Saturation distribution according to the Buckley-Leverett model [11].

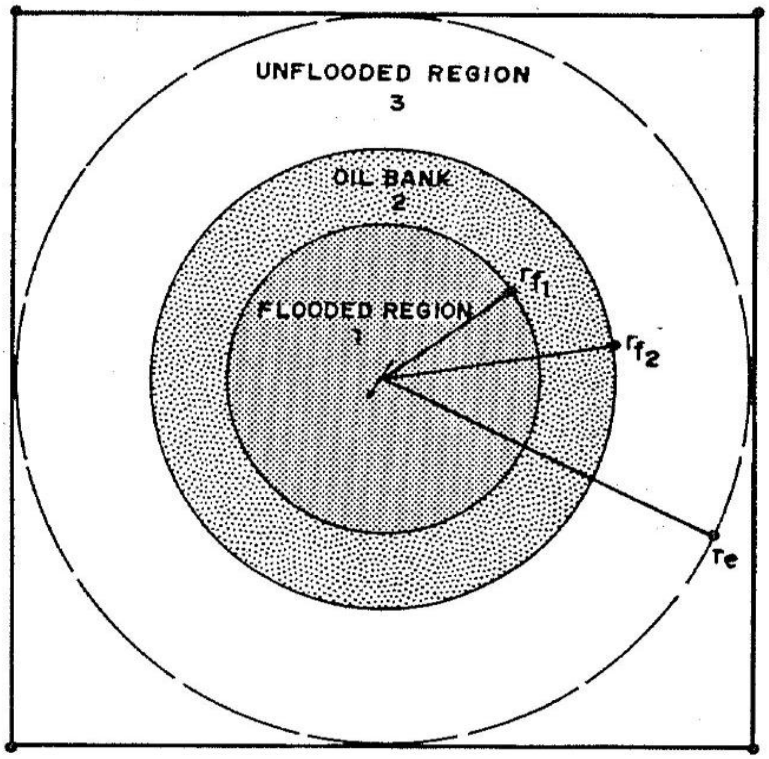

Figure 5: Plan view of saturation distribution around injection well [12].

The displacement can be characterized based on the value of the mobility ratio (M) described as follows:

M<1 → Piston like displacement, narrow transition zone and high recovery efficiency.
M=1 → Weak piston like displacement, transition zone of moderate width and moderate recovery efficiency.
M>1 → Large transition zone, low recovery efficiency.

A composite reservoir would be seen if the transition zone is eliminated from Figure 4 and Figure 5 causing sudden change in saturation after the flood out zone. Abrupt, radial changes in permeability can also be described as a composite reservoir [**11**].

2.5 Injection and Falloff tests

2.5.1 Hazebroek, Rainbow, and Matthews method

Hazebroek, et al. in 1958 [**6**] obtained analytical solution for the pressure falloff tests in water injection wells. For the case of unit mobility ratio, they proved that this method gave the same results for permeability thickness product as the conventional build-up method. This new method gave correct values for static pressure as compared to the conventional method. Their study was based on assumptions as follows:

- Outer boundary of the oil and water bank are of circular cross section
- Saturation changes abruptly in each zone at the boundaries
- Pressure at the outer boundary remains constant
- Front remains stationary throughout the falloff test and a constant pressure at the front.

They studied two different cases where oil and water have the same properties and they have different properties.

2.5.2 Kazemi, Merill and Jargon

Kazemi, Merill and Jargon [**13**] investigated the pitfalls of pressure falloff analysis in reservoirs with and without fluid banks. Pressure-time data from a falloff test yield information about many parameters, but to interpret actual falloff test data from a field is very difficult. They suggested that by pressure falloff the front tracking or locating discontinuities and determining transmissibility's must be done with extreme caution as the curve reflection might indicate some other phenomena. They used numerical simulation to investigate this problem and came out with following conclusions:

- Slopes of the falloff curve are influenced by mobility ratio, after flow and specific storage ratio and the changes in slope are often erroneous because of fluid bank or transmissibility change due to changes in permeability near the wellbore.
- Early time data would give proper transmissibility results if the afterflow effects are minimized.
- Even though the front does not remain stationary during the tests Horner plot can be used to interpret falloff tests, as the compressibility of oil is greater than that of the invaded zone which reduces the frontal advance rate during the test.
- If the specific storage, ϕC_t of the water zone is equal to that of the invaded zone, and the front radial distance is at least 10 times the radial distance of the invaded zone then the slope of the second straight line is proportional to the transmissibility of the invaded zone.
- Falloff test cannot be interpreted if the wellbore storage constant calculated from field data, C, exceeds the physical reality of the system.

2.5.3 Merill, Kazemi, and Gogarty

Merill, Kazemi and Gogarty [**12**] studied the pressure falloff tests in two and three zone systems. Their investigation was based on the above model discussed i.e [**13**]. They discussed various shapes of curves for a two zone system that could be obtained during a pressure falloff test when M>1, M=1 and M<1. Figure 6 shows

dimensionless pressure plotted against dimensionless time only for M>1 other graphs of M=1 and M<1 are explained in [**12**]. The curves were divided into four sections:

- Section A – Time span dominated by wellbore storage
- Section B – Time span within which the slope is determined by the properties of the water zone
- Section C – Transition period
- Section D – Time span during which slope is controlled by the properties of water zone and the uninvaded zone.

Dimensionless plots were generated using the following equations:

$$P_D = \frac{\lambda_1 h(P_i - P_{ws})}{70.6qB} \qquad \text{Eq (2.18)}$$

λ_1 = mobility of water zone

$$\Delta t_{Df1} = \frac{2.637 * 10^{-4}\lambda_1 \Delta t}{(\emptyset C_t)_1 r_{f1}^2} \qquad \text{Eq (2.19)}$$

$(\emptyset C_t)_1$ = Specific storage of the water zone

r_{f1} = Distance of the injection well to the nearest front, feet

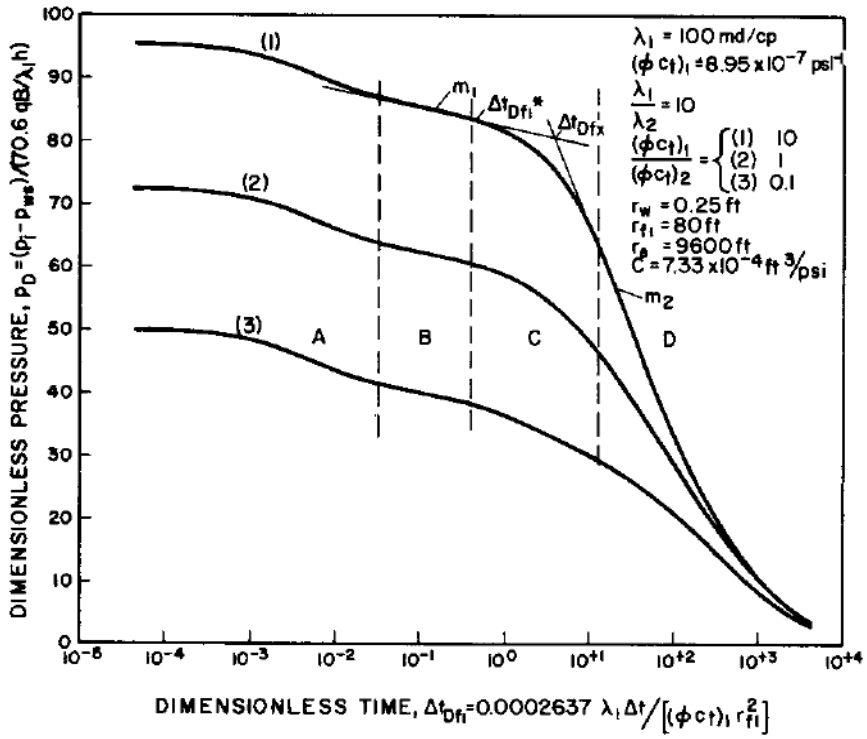

Figure 6: Simulated pressure falloff for a two zone system, Mobility ratio greater than 1 [**12**]

From numerous computer runs for various specific storage ratios, mobility ratios and radius of invaded zone Merill, et al. [**12**] produced a cross plot of slope ratio m_2/m_1 and mobility ratio λ_1/λ_2 as shown in Figure 7 below. From the figure if the specific storage ratio $(\emptyset C_t)_1/(\emptyset C_t)_2$ = 1, then the slope ratio will be equal to the mobility ratio. And if the specific storage ratio is other than 1, then the mobility ratio can be estimated from Figure 7. Radial distance to the front could also be calculated by using the following equations given below:

$$r_{f1} = \sqrt{\frac{0.0002637\ \lambda_1\ \Delta t_{fx}}{(\emptyset C_t)_1\ \Delta t_{Dfx}}} \qquad \text{Eq (2.20)}$$

$$r_{f1} = \sqrt{\frac{5.6146\ q_w t_{inj} B_w}{\pi h \emptyset \Delta S_w}} \qquad \text{Eq (2.21)}$$

Δt_{Dfx} is determined by the plot of correlation for dimensionless intersection time as shown in Figure 8 [**12**]

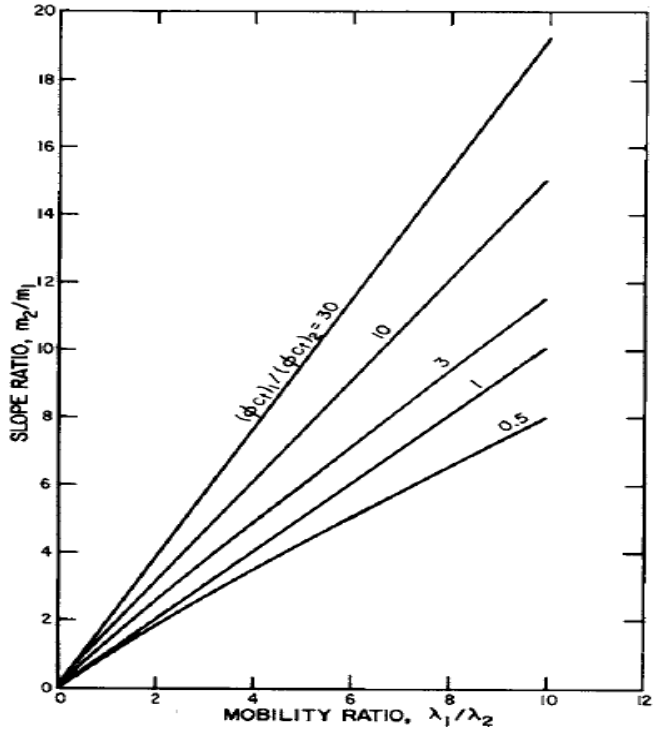

Figure 7: Cross plot of slope ratio, m_2/m_1, and mobility ratio, λ_1/λ_2 [12]

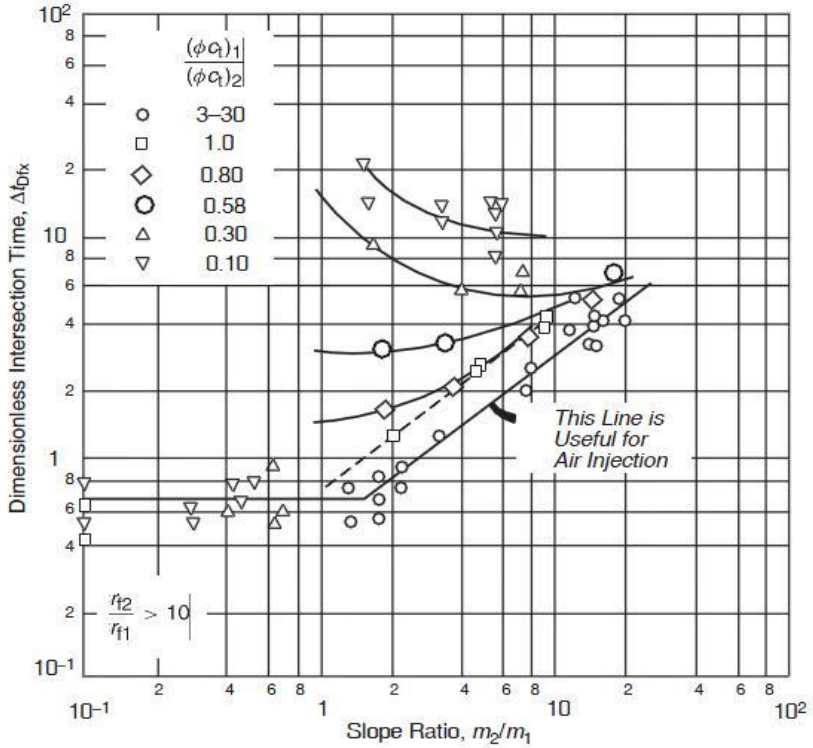

Figure 8: Correlation of dimensionless intersection time, Δt_{Dfx} for falloff data from two zone reservoir [13].

The authors [**12**] finally concluded that for water flood systems for two zones, pressure falloff tests could yield the distance to the front, mobility and saturation for both invaded and uninvaded zones as compared to the gas injection systems which could determine mobility of the invaded zone only and distance to the front. In a three zone system the only information which could be obtained is the mobility of the invaded zone.

2.5.4 Sosa, Raghavan, and Limon

Effect of relative permeability and mobility ratio on pressure falloff behavior was studied by Sosa, et al. in the year 1981 [**14**]. Objectives of this study are listed as below.

- To analyze and study the effect of saturation gradient on pressure falloff tests.

- To describe the movement of fluid banks that have been proposed by Hazebroek, et al. [**6**] and Kazemi, et al. [**13**] which assume that composite zones are developed as a result of fluid injection, and abrupt changes in mobility occurs at the interface of each zone.

A numerical simulation model was developed to investigate the pressure falloff tests and considered two sets of relative permeability data and six values of mobility ratio was examined using a semi-implicit procedure to solve finite difference equation. Shut in pressure vs. Horner time function and saturation vs. radial distance profiles were generated for all the simulation runs and concluded that from a falloff test distance to the front cannot be determined. The injection time and mobility ratio M affect the shape of the pressure falloff curve.

If two straight line segments appear on the curve for M=1 then the slope of the first straight line estimates the mobility of water at residual oil saturation, which is similar for cases where M<1 and M>1 which is in agreement with the previous models discussed. And the average water saturation behind the front is determined by analyzing the slope of the second straight line. If M<1 total mobility of the system is obtained from the slope of the second straight line. If M>1 no specific value of water saturation could be assigned to the second straight line slope.

2.5.5 N-S. Yeh and R.G. Agarwal

Yeh and Agarwal [**7**] used simulators and examined large number of scenarios to examine pressure transient analysis of injection wells in reservoirs with multiple banks. The principle objective of this study was to develop a systematic approach for analyzing well test pressure data and to calculate mobility profile, fluid bank radii, and pressure distribution in the reservoir. They also studied the effects of various parameters on pressure response such as, relative permeability, viscosity effect, initial water saturation, compressibility effect, real skin effect and wellbore storage effect.

Yeh and Agarwal studied the pressure response for injection and falloff tests as shown in Figure 9 and Figure 10 by using the injection response and derivative plot they estimated the total mobility (λ_t) of the water zone, using the following equation:

$$\lambda_t = \frac{70.6qB}{h\Delta P'_{wf}} \qquad \text{Eq (2.22)}$$

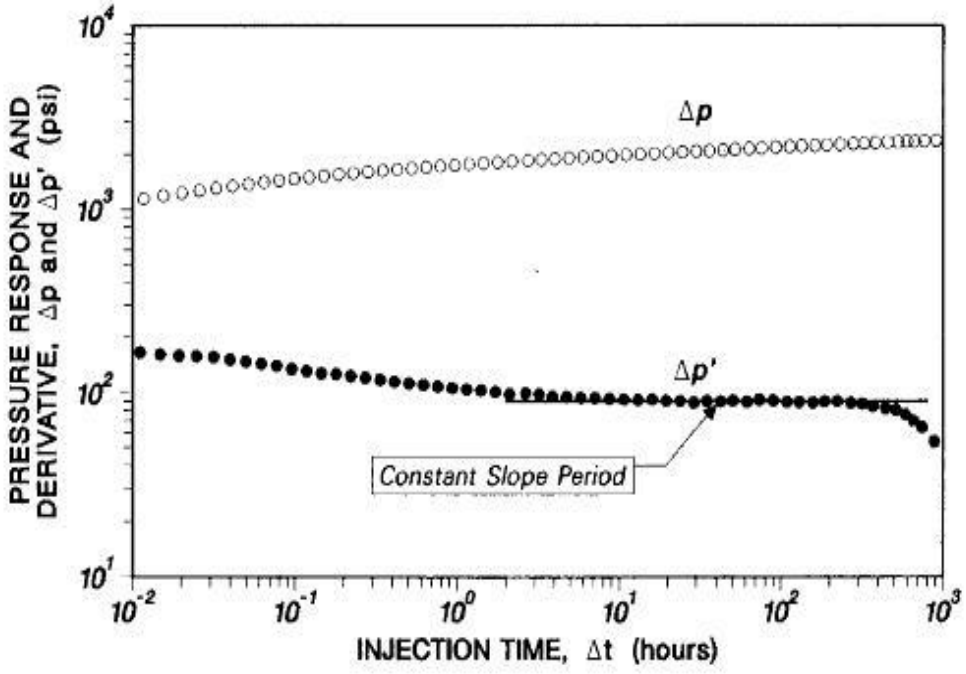

Figure 9: Injection pressure response and derivative curve [7]

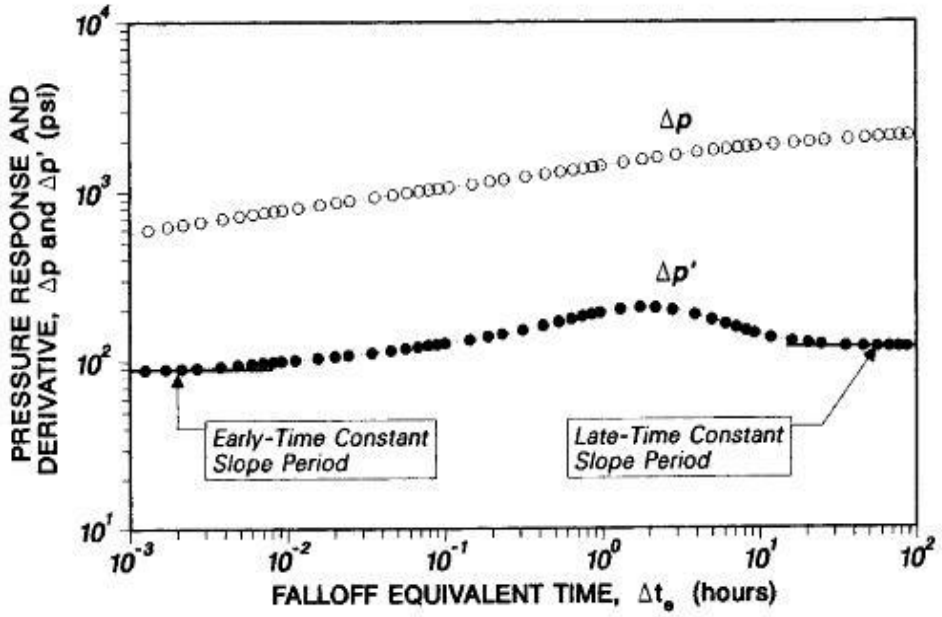

Figure 10: Falloff pressure response and derivative curve [7]

By using the Falloff pressure response and derivative curve, Yeh and Agarwal estimated, volumetric average of total mobility as a function of radial distance r from the equation given below, and the distance to the front was estimated form the plot of total mobility profile shown in Figure 11

$$r = 0.024\left[\frac{\lambda_{tavg}\Delta t_e}{\emptyset c_t}\right]^{0.5} \qquad \text{Eq (2.23)}$$

$$\lambda_t = \frac{r}{2}\frac{d\lambda_{tavg}}{dr} + \lambda_{tavg} \qquad \text{Eq (2.24)}$$

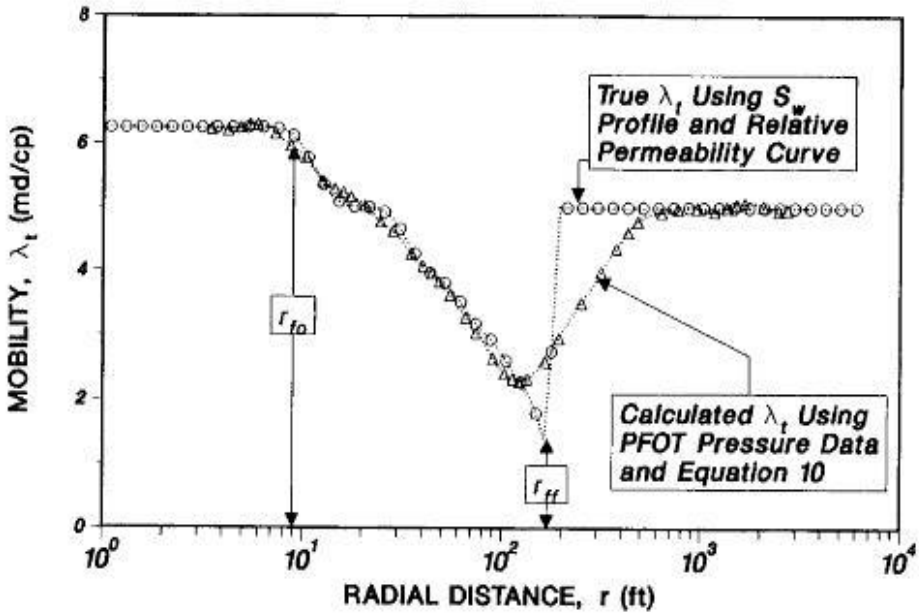

Figure 11: Reservoir mobility profile to determine r [7]

Yeh and Agarwal concluded that the new analysis method is applicable to a range of mobility ratios and is independent of the availability of relative permeability. And also they pointed out that, to interpret the falloff curves, the pressure data should be free from noise and the pressure derivative curves obtained from high permeability reservoirs could be meaningless as the falloff could be very small, unless the injection rate is very high.

2.5.6 Noaman A.F. El-Khatib

Noaman El-Khatib [**15**] studied transient pressure behavior for well under natural water drive with moving boundaries. He solved simultaneous equations in Laplace space using finite difference method to estimate the location of moving front iteratively, and then used Stehfest algorithm to investigate effects of reservoir size, aquifer size, production rate, mobility ratio, skin, and wellbore storage in real time domain by plotting dimensionless pressure and derivative vs. dimensionless time. The equations used in his work are as shown below:

$$P_D = \frac{2\pi h \lambda_1 (P_i - P)}{qB} \quad \text{Eq (2.25)}$$

$$P'_D = \frac{dP_D}{dlnt} = t\left(\frac{dP_D}{dt}\right) \quad \text{Eq (2.26)}$$

He showed that the composite reservoirs behave as infinite homogeneous reservoirs until the external boundary is felt which is around 10^5 dimensionless time and from this time the dimensionless pressure may decline. Storativities were found to have little effect on the pressure curves, whereas wellbore storage, skin, mobility and aquifer radius influenced the pressure behavior.

2.5.7 Michael M and Levitan, BP

Michael M. Levitan, BP [**16**] in 2002 presented a new analytical method for accurate solution of the pressure transient problem for two-phase flow associated with water injection/falloff tests. The algorithm developed allowed to compute the solutions for any step-wise constant rate sequence that includes multiple injection and falloff periods.

They considered a two-phase non-isothermal flow problem associated with water injection to analyze saturation and temperature profiles. The equations generated for combined fluid flow and heat transfer problems could not be solved analytically. Hence assumptions were made based on Buckley-Leverett fluid displacement model and convective mechanism of heat transfer to develop analytical solutions. They found out that the saturation and the temperature solutions were valid for any injection rate vs. time function.

They also considered the pressure transient problem during water injection/falloff test sequence governed by the following equation.

$$c_d(S_w)\frac{\partial p_d}{\partial t_d} = \frac{1}{r_d}\frac{\partial}{\partial r_d}\left[\lambda_d(S_w) r_d \frac{\partial p_d}{\partial r_d}\right] \quad \text{Eq (2.27)}$$

Analytical solution developed using the above equation was difficult to solve because of the presence of the convection term in the derived equation, hence considerations of step-wise constant rate functions which is a rate approximation constantly used in well test analysis was used to simplify the equation. They also noticed that at early time region, the pressure curve reflects the properties ahead of the front, and at late time it reflects the properties close to the well in the region behind the front. This pressure regime was termed as self-similar regime. In this self-similar regime, the well pressure derivative developed a horizontal trend at late time and the value of the derivative is inversely proportional to the mobility in the water-invaded zone. The pressure at the front is also constant. This constant pressure at the front shielded the region behind the front and the well pressure derivative depended only on the flow properties in the water-invaded zone.

They also studied this self-similar regime in depth by considering different pressure trends caused by variable injection rate and falloff periods. In a way self-similar regime "contradicted" the concept of radius of investigation. As the time increases the bottom hole pressure reflects the reservoir properties further and further away from the well which is however not the case with constant rate injection. This self-similar regime does not begin immediately with the start of injection period. It takes some time after a change to a new rate for the self-similar regime to develop. Hence some transition period always precedes the onset of the self-similar regime and the duration of this transition period depends on the size of the water-invaded zone at the time of rate change and the pressure field around the well that exists prior to the rate change. Smaller the water invaded region the shorter the transition period.

At the very beginning of the water injection, when initially there is no water bank, the pressure transient almost immediately moves into the oil zone ahead of the water front. This is the main reason why the early time pressure derivative reflects the oil zone mobility. But during the falloff period when injection is stopped, the water front also stops and saturation changes are also insignificant. As a result, pressure behavior during the early time, reflects the fluid mobility in the water zone near the well, and at late time, it reflects the fluid mobility in the oil zone ahead of the flood front.

2.5.8 Amina A. Boughrara and Alvaro M. M. Peres

Amina et al. [**17**] in 2006 used Thompson-Reynolds steady-state theory to construct approximate analytical solutions for injection wellbore pressure at vertical and horizontal water injection wells. They added a two-phase term to a single-phase solution that represents the existence of a two-phase zone and the movement of the water front. They first presented a solution for an isotropic reservoir and from there obtained solution for an anisotropic reservoir by introducing a coordinate transformation.

They generated approximate analytical solutions for the injection pressure at vertical and horizontal water injection wells. By comparison with a numerical solution generated from a reservoir simulator, they showed that the analytical solutions gave sufficiently accurate solutions for practical purpose. As a skin zone of even a few inches in radius could have a dominant effect on the injection pressure solution, the solutions are based on a thick skin modeled by Hawkins formula. These models proved useful for both, understanding the pressure derivative behavior during injection tests and for analyzing injectivity tests using nonlinear regression to determine permeability and the skin factor to determine if it was necessary to simulate the well to obtain the desired injectivity. Moreover, these analytical solutions were necessary to construct falloff solutions.

For radial flow case, they have provided a rigorous explanation of why the injection pressure may reflect endpoint oil mobility at early times prior to exhibiting a semi-log straight line inversely proportional to endpoint water mobility.

The pressure derivative for the restricted-entry solution could remain negative throughout a long injectivity test. They have shown this using the analytical solution and verified it by comparison with numerical solutions.

When water was injected into a completely-penetrating well near a fault, the pressure derivative exhibited the classical response based on a doubling of slope. Instead the pressure derivative increases by a factor of (1+M) where M denotes the endpoint mobility ratio and finally concluded that the solution for isotropic reservoir could be

extended to an anisotropic system by applying a spatial transformation to convert the anisotropic system to an equivalent isotropic system.

CHAPTER 3

METHODOLOGY

This chapter describes the methods that will be followed through to achieve the objectives of the project. The description of the process to be followed for the completion of this work is explained as follows:

3.1 ECLIPSE 100

Schlumberger ECLIPSE 100 software is used in this project to generate a simulation model, Assuming 1 dimensional radial homogeneous model with 1 injection well at the centre, penetrating the whole layer, and neglecting gravity effects. Input data to the simulation model is mainly taken from [**7**] and is shown in Table 1.

3.2 Pressure transient study

Interpreting and analyzing the results (Pressure vs. Time, saturation profile, reservoir pressure profile etc.) obtained from ECLIPSE 100 software has to be carried out until the end of this project to achieve the desired objectives.

Once the literature survey is completed, methodology to be followed to achieve the desired objectives is as shown below:

1. Simulation model is to be generated using ECLIPSE 100 simulation software.
2. Simulation has to be carried out for both injection and falloff tests.
3. Pressure vs. time data from the simulation model should be obtained for injection and falloff tests.
4. Parameters such as, skin, permeability and mobility is to be estimated using semi-log plot of pressure vs. time obtained from step 3.

5. Mobility profile is to be generated, studied and compared using the derivative plot and saturation profile.
6. Saturation profile is to be obtained and analyzed from the simulation model ECLIPSE 100.
7. Estimation of the distance to the leading edge of the water bank should be made using equations provided in the literature.
8. Parameters mentioned in the objectives are to be changed to study the pressure behavior.

Overall flowchart of the methodology to be followed is provided below:

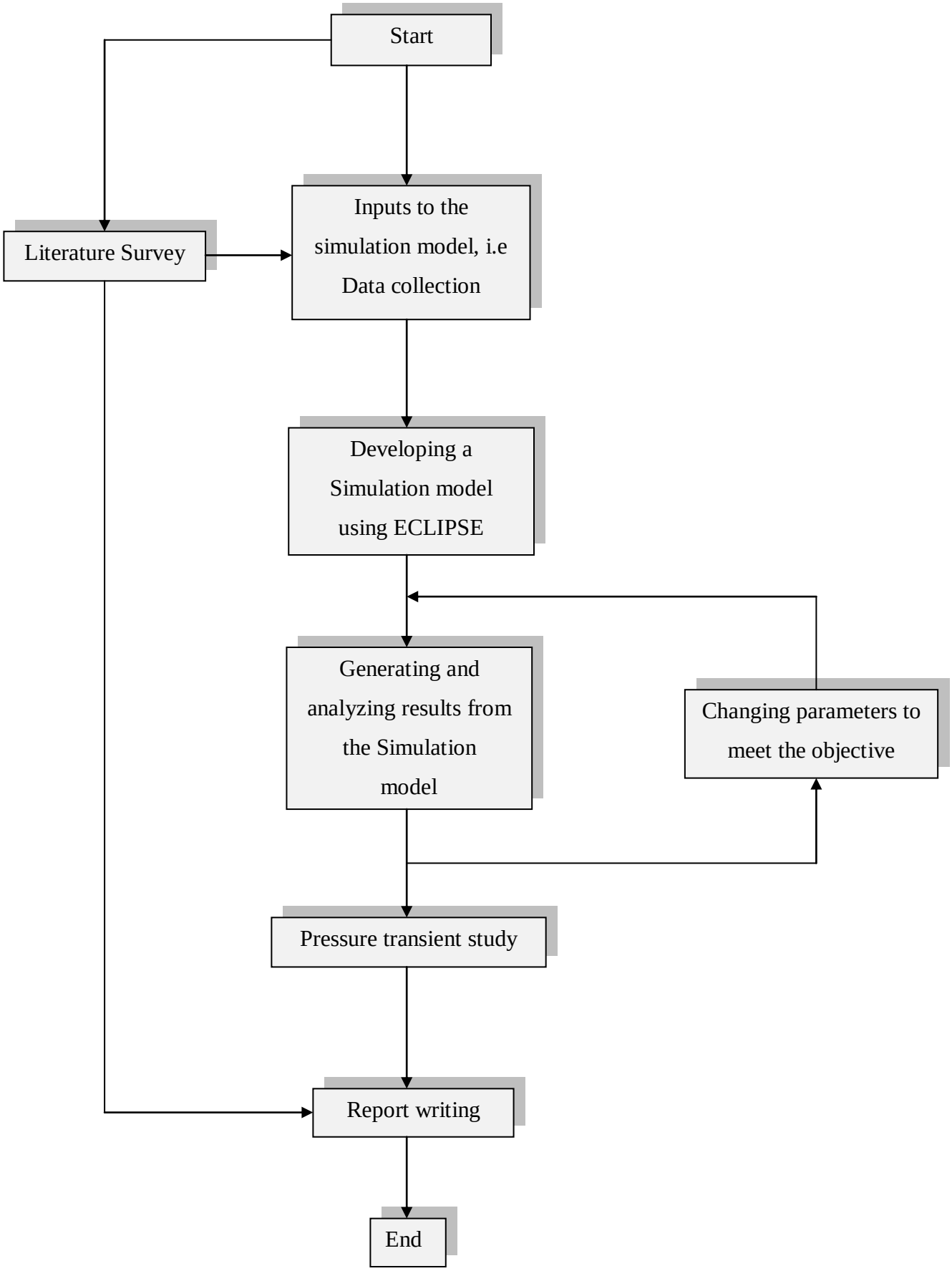

CHAPTER 4

RESULTS AND DISCUSSION

This chapter deals with the description of the model used, input data to the simulation model and finally the results obtained to investigate the pressure transient analysis of injection wells during injection and falloff periods.

4.1 Simulation Model

One dimensional radial homogeneous model of 210*1*1 grids were used for this study. Small sized girds were placed in the r direction near the well bore and the gird sizes were increased away from the wellbore. 1 injection well was placed at the centre, penetrating the whole layer, gravity effects were neglected and the model was generated using Schlumberger ECLIPSE 100. Simulation studies were conducted in this model with an external reservoir radius of 1500 ft and a layer thickness of 100 ft. Absolute permeability and porosity is constant throughout the reservoir. Capillary pressure was assumed to be zero. Initial reservoir pressure is 600 psia. Injection well was located in the cell (1, 1, 1). The perforation thickness of the well was equal to the reservoir thickness of 100 ft. Figure 12 shows the radial 1D model used for numerical simulations.

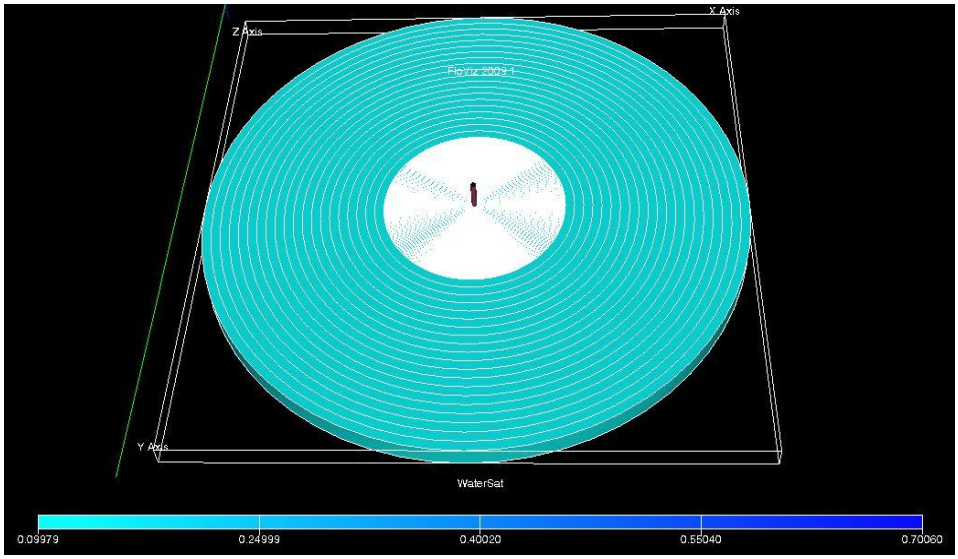

Figure 12: Radial 1D model

Water was injected for 10 days starting from 01 JAN 2012 to 11 JAN 2012, followed by a shut-in period of 10 days starting from 11 JAN 2012 to 21 JAN 2012. The reservoir was pressurized initially during the injection period with a constant injection rate, 200 stb/day.

4.2 Input data

Input data to the simulation model is mainly taken from [7]. Table 1 below shows the data used for this project.

Table 1: Rock and fluid properties and well conditions for base case

Initial Reservoir Pressure, P_i	600 psi
Initial Water Saturation, S_{wi}	0.1
Reservoir Thickness, h	100 ft
Reservoir External Radius, r_e	1500 ft
Porosity, Φ	0.1
Absolute permeability, k	10 md
Compressibility of oil, C_o	3 E-05 psi^{-1}
Compressibility of water, C_w	3 E-06 psi^{-1}
Viscosity of oil, μ_o	10.0 cp
Viscosity of water, μ_w	0.4 cp
Wellbore radius, r_w	0.5 ft
Injection time, t_{inj}	10 days
Injection rate, q_w	200 bwpd

Relative permeabilities are generated using the following Corey's equations:

$$k_{rw}(S_w) = \left(k_{rw,max}\right) * S_{wD}^4 \qquad \text{Eq (4.1)}$$

$$k_{ro}(S_w) = (1 - S_{wD}^2) * (1 - S_{wD})^2 \qquad \text{Eq (4.2)}$$

Where

$$S_{wD} = \frac{S_w - S_{wc}}{1 - S_{or} - S_{wc}} \qquad \text{Eq (4.3)}$$

$$S_{wc} = S_{wi} = 0.1,\ S_{or} = 0.3\ and\ k_{rw,max} = 0.25$$

Total mobility λ_t as a function of water saturation S_w is calculated using the following equation:

$$\lambda_t = k\left(\frac{k_{ro}}{\mu_o} + \frac{k_{rw}}{\mu_w}\right)_{s_w} \qquad \text{Eq (4.4)}$$

The relative permeability and total mobility curves generated using the above equations, are shown in Figure 13 below, and Table 5 Appendix A, shows the relative permeability and mobility values used in the simulation model.

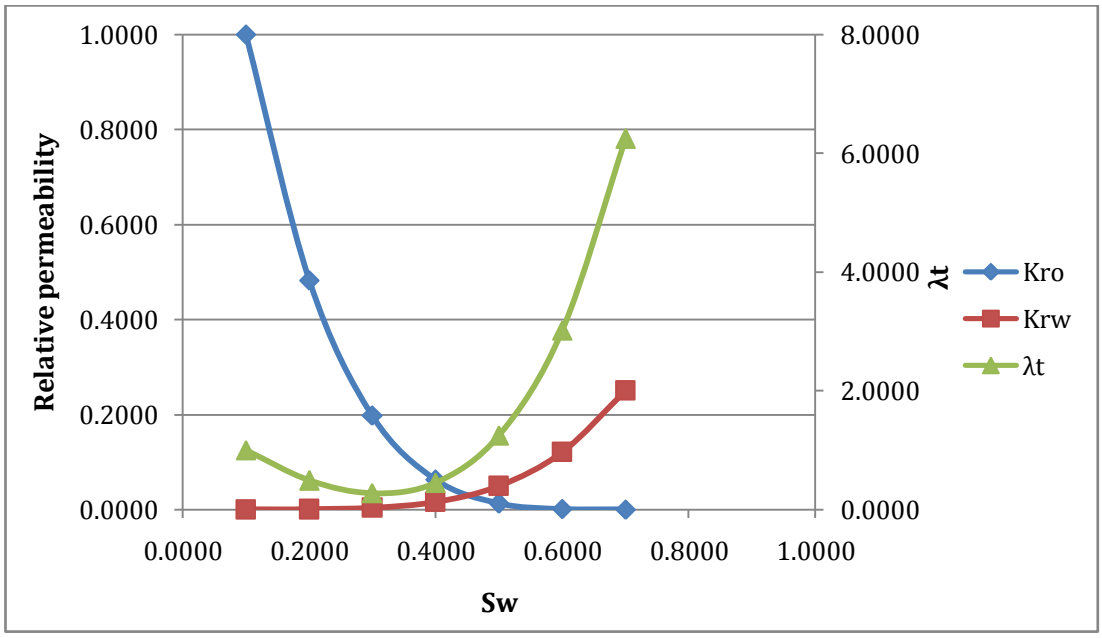

Figure 13: Relative permeability and Total mobility vs. Saturation

Initially results obtained for the input data mentioned in Table 1 were generated using the ECLIPSE 100 simulation model with zero wellbore storage and skin effects, and pressure transient studies are done using Microsoft Excel. Detailed studies are done for the initial case followed by studying the effects of changing few parameters in the input data which are discussed later in this chapter.

4.3 Initial Results

Using the data mentioned in Table 1, a 1D simulation model is generated using 210 grids in the r direction and the size of each grid is distributed in a manner where, small gird blocks are used near the wellbore, and becomes coarser away from the wellbore. 0.5 ft grid spacing (dr) is used for the first 100 grids blocks followed by 5 ft grid spacing for the next 90 grids and finally 50 ft spacing for the last 20 grids. Thus, total radial distance from the wellbore to the boundary is 1500 ft. The mobility of oil and water used in the simulation model is shown below:

Mobility of water

$$\lambda_w = \left(\frac{kk_{rw}}{\mu_w}\right)_{s_{wc}} = \frac{10 * 0.25}{0.4} = 6.25$$

Mobility of oil

$$\lambda_o = \left(\frac{kk_{ro}}{\mu_o}\right)_{S_{or}} = \frac{10 * 1}{10} = 1.0$$

4.3.1 Injection analysis

Figure 14 shows the BHP plotted against injection time from ECLIPSE. The bottom hole pressure increases with time when water is injected at a constant injection rate of 200 stb/day. The plot shows an injection period of 240 hrs i.e 10 days.

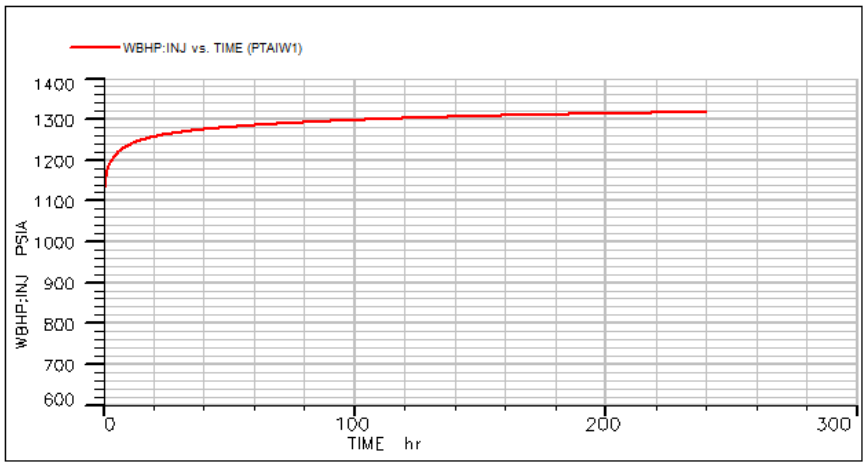

Figure 14: Injection pressure response, Bottom hole pressure vs. Time (hr)

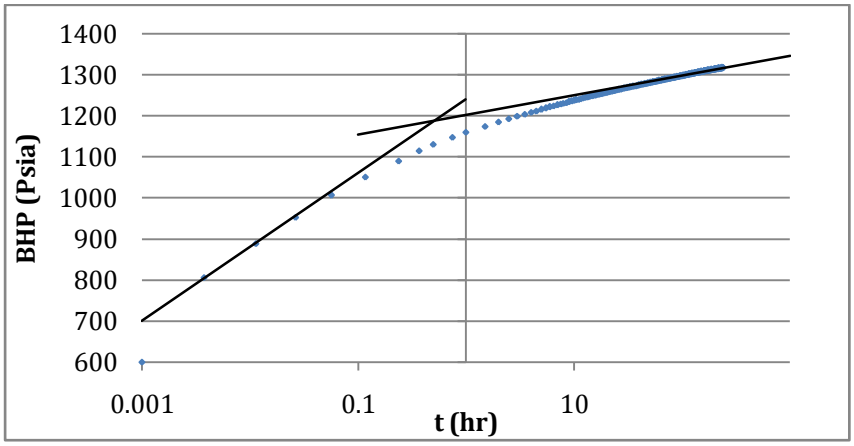

Figure 15: Injection pressure response, Bottom hole pressure vs. Injection time (hr) semi-log plot

Further studies are carried out when BHP is plotted against logarithm of injection time i.e semi-log plot as shown in Figure 15. Since there is no influence of wellbore storage and skin in this semi-log plot, the two tangents should estimate the skin, permeability and mobility of oil and water zones.

From the Semi-Log plot of BHP vs. injection time, analysis of the slope, skin, permeability and mobility are shown below:

Slope of the first and second tangent line was found to be, m1 = 180 and m2 = 48

$$M_w = \frac{k_w}{\mu_w} = \frac{162.6qB_w}{m_1 h} = \frac{162.6 * 200 * 1}{48 * 100} = 6.775 \text{ md/cp}$$

$$M_o = \frac{k_o}{\mu_o} = \frac{162.6qB_o}{m_2 h} = \frac{162.6 * 200 * 1}{180 * 100} = 1.80 \text{ md/cp}$$

$$k_w = \frac{162.6\text{qB}_\text{w}\mu_\text{w}}{\text{m}_1\text{h}} = \frac{162.6*200*1*0.4}{48*100} = 2.71 \text{ md}$$

$$s = 1.151\left[\frac{P_{1hr} - P_i}{m} - Log\left(\frac{k}{\Phi\mu C_t r_w^2}\right) + 3.23\right] = -0.04$$

Skin obtained is almost zero which is in consistent with the input data, but the mobilities obtained from the injection analysis differ from that of the input data which is due to the movement of oil and water banks, as the water bank continues to move radially outwards from the wellbore which is proportional to injection time.

Figure 16 shows the log-log plot of injection pressure difference ($P_{wf} - P_i$) and derivative curve ΔP' plotted against injection time. The derivative curve ΔP' is a derivative of pressure difference ΔP with respect to natural logarithm of time. The derivative values obtained to generate the curve are shown in Table 6 Appendix A, with an example calculation.

$$\Delta P' = \frac{d\,\Delta P}{d\,ln(\Delta t)} \qquad \text{Eq (4.5)}$$

ΔP' is not constant during the injection period but varies with respect to time, this is because of the two phase flow effects in the reservoir. Hence injection test pressure response cannot be used directly to obtain the properties of the oil bank or uninvaded zone [**7**].

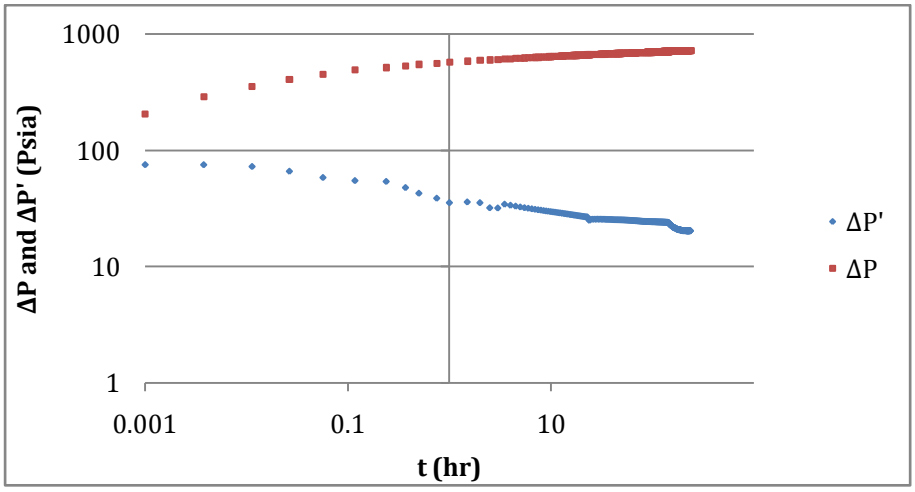

Figure 16: Injection pressure response, Pressure change and derivative vs. Injection time (hr) log-log plot

4.3.2 Falloff analysis

Figure 17 shows the plot of BHP vs. time generated from ECLIPSE. The graph shows a smooth increase of BHP during the injection period and then after 240 hrs of water injection the well is shut-in for again 240 hours. A decline in BHP is noticed from 240hrs - 480 hrs.

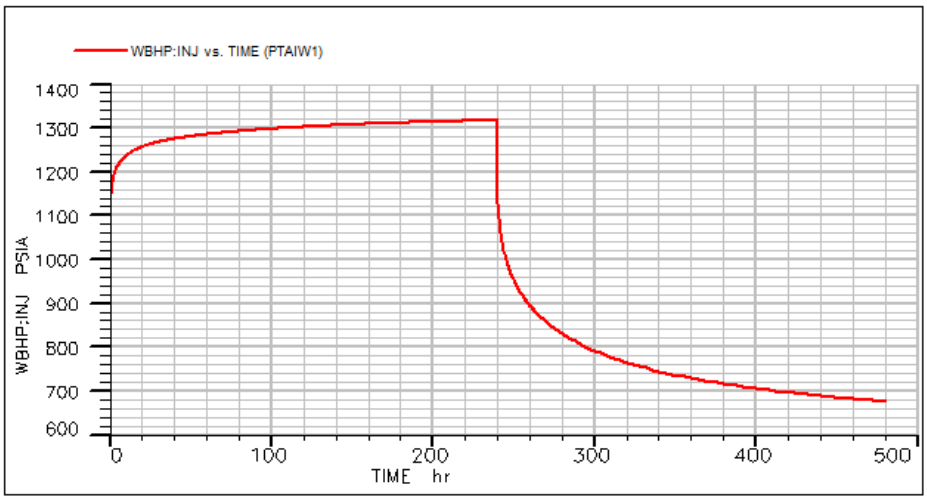

Figure 17: Falloff pressure response, Bottom hole pressure vs. Time (hr)

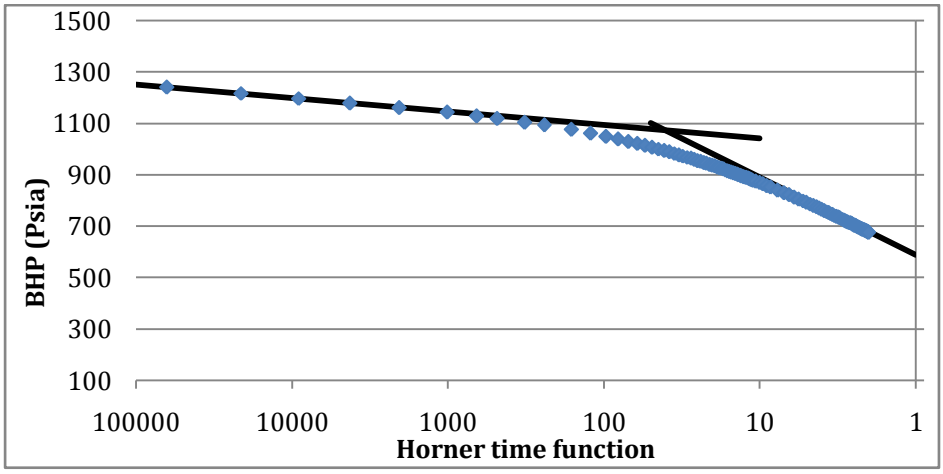

Figure 18: Falloff pressure response, Bottom hole pressure vs. Horner time function

Figure 18 above shows a plot of BHP against Horner time function $(t_p + \Delta t)/\Delta t$, for falloff pressure response. This semi-log plot exhibits a straight line with intercept P^* at infinite shut-in time i.e Horner time of 1. This extrapolated pressure P^* is equivalent to the initial reservoir pressure P_i for infinite acting reservoir. From the plot we can see the extrapolated pressure to be 600 Psia which is equal to the initial reservoir pressure.

From the Semi-Log plot of BHP vs. Horner time function, analysis of the slope, skin, permeability and mobility are shown below:

Slope of the first and second tangent line was found to be, m1 = 52 and m2 = 301.95

$$M_w = \frac{k_w}{\mu_w} = \frac{162.6qB_w}{m_1 h} = \frac{162.6 * 200 * 1}{52 * 100} = 6.254 \text{ md/cp}$$

$$M_o = \frac{k_o}{\mu_o} = \frac{162.6qB_o}{m_2 h} = \frac{162.6 * 200 * 1}{301.95 * 100} = 1.077 \text{ md/cp}$$

$$k_w = \frac{162.6\text{q}\text{B}_\text{w}\mu_\text{w}}{\text{m}_1\text{h}} = \frac{162.6 * 200 * 1 * 0.4}{52 * 100} = 2.501 \text{ md}$$

$$s = 1.151\left[\frac{P_{wf} - P_{1hr}}{m} - Log\left(\frac{k}{\Phi\mu C_t r_w^2}\right) + 3.23\right] = 0.019$$

Skin obtained is almost zero which matches with the input data. The mobilities obtained also compares very well with the actual input mobility values of oil and water, these consistencies in obtaining a good match for all the parameters being calculated is due to the stationary banks during the falloff period.

Figure 19 shows a log-log plot of pressure difference ΔP ($P_{wf,s} - P_{ws}$) and pressure derivative ΔP' against falloff equivalent time (Δt_e). The derivative curve ΔP' is a derivative of pressure difference ΔP with respect to natural logarithm of time and is given by Eq 31, and the falloff equivalent time is analogous to the buildup equivalent time.

$$\Delta t_e = \frac{t_i * \Delta t}{t_i + \Delta t} \qquad \text{Eq (4.6)}$$

Where Δt is shut-in time, hrs and t_i is the total injection time, hrs.

The reflection of radial flow in the flooded zone (water bank) and the unflooded zone (oil bank) is shown by two constant slopes from the derivative curve ($\Delta t_e \leq 0.2$ hrs) and ($\Delta t_e \geq 6$ hrs) respectively. These slopes represent constant mobility zones for oil and water banks. It is also important to note that normally during actual field tests the early time period is obscured by wellbore storage effects which in this case is zero hence a smooth constant slope of early time period is obtained. Sometimes constant slope of the unflooded zone (oil bank) during a field test may not be displayed if the test duration is not long enough or the boundary effects become dominant. During the transition period there are saturation changes $S_{wi} \leq S_w \leq (1\text{-}S_{or})$ and the total mobility does not remain constant but changes with saturation gradient.

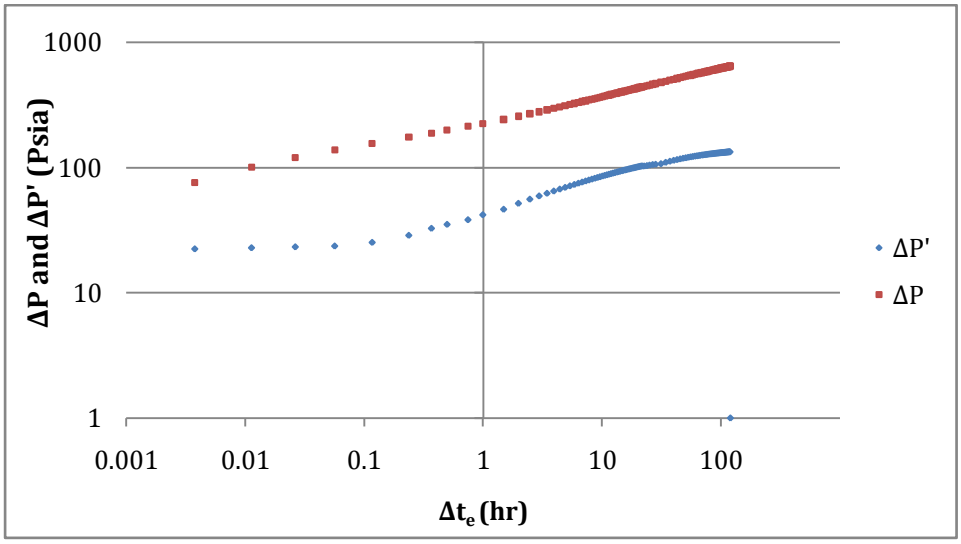

Figure 19: Falloff pressure response, Pressure change and derivative vs. falloff equivalent time (hr)

4.3.3 Reservoir pressure profile & saturation profile

Figure 20 shows the reservoir pressure profile after 1, 2, 5 and 10 days of injection time. Reservoir pressure is almost equal to the bottom hole pressure closer to the wellbore and reduces as pressure diffuses away from the wellbore. Since our model represents a line source solution with the applicability of an infinite acting reservoir system, the pressure profile eventually reaches the initial reservoir pressure, 600 Psia. This is due to the pressure not reaching the external boundary of the reservoir.

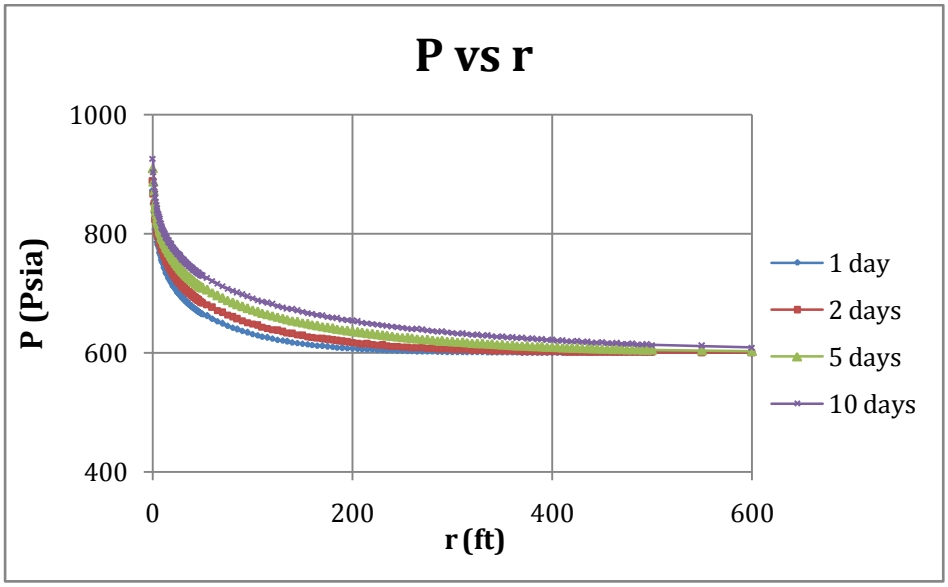

Figure 20: Pressure vs. Radial distance

Figure 21 shows the saturation profile obtained from ECLIPSE at the end of 1, 2, 5 and 10 days of injection time. This figure illustrates the flood out zones being formed ($S_w = 1–S_{or} = 0.7$) during the injection period, and a sharp change in water saturation indicating the flood front which moves away from the well as injection time increases. The region where $S_w = 1–S_{or} = 0.7$ and $S_w = S_{wi} = 0.1$ will yield the mobility of the flood out zone and the unflooded zone respectively. The region of water saturation S_w in-between $1\text{-}S_{or}$ and S_{wi} is the transition zone where saturation changes and as a result, mobility changes with saturation gradient. Figure 22 shows water saturation plotted against square of the radial distance. As the injection time doubles from 1-2 days and 5-10 days, the area under the curve also almost doubles giving an impression of how the saturation changes occur when plotted against r^2.

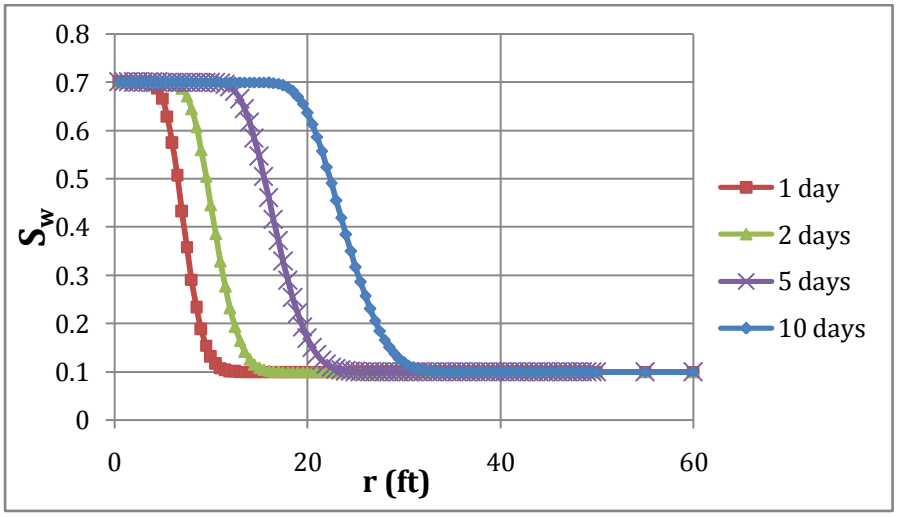

Figure 21: Saturation vs. Radial distance

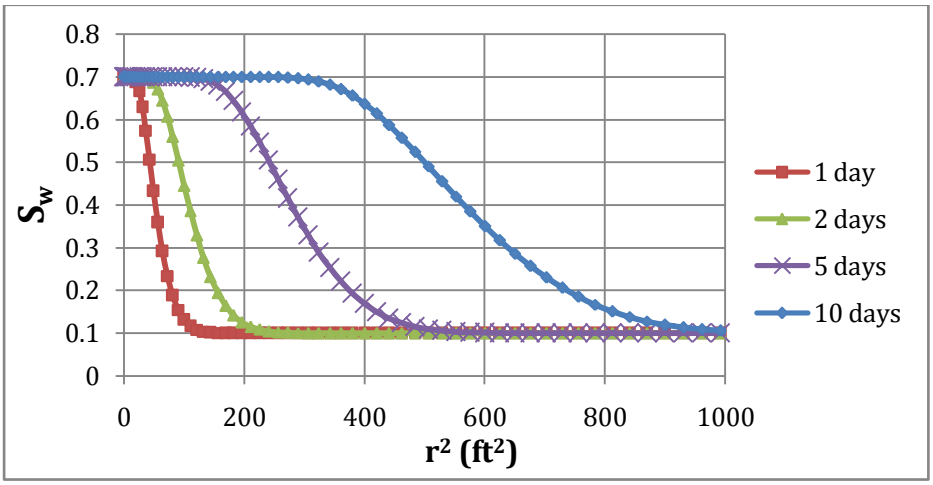

Figure 22: Water saturation vs. Radial distance square

4.3.4 Total mobility estimation

Using the equations Eq (2.22) and Eq (2.23), total mobility plot from the derivative curve is generated against radial distance representing the flood out zone (water bank) and the unflooded zone (oil bank). There exists a transition zone between the two zones, where the total mobility reduces as a function of radial distance due to the changes in the saturation gradient. From Figure 23 it is clearly observed that, the total mobility profile follows the curve of water saturation profile generated from ECLPISE at the end of falloff period (20 days). Table 7 Appendix A, shows a trial calculation for the total mobility calculated from the derivative curve.

$$\lambda_t = \frac{70.62qB}{h\Delta p'}$$

$$r = 0.024\sqrt{\frac{\lambda_t \Delta t_e}{\emptyset C_t}}$$

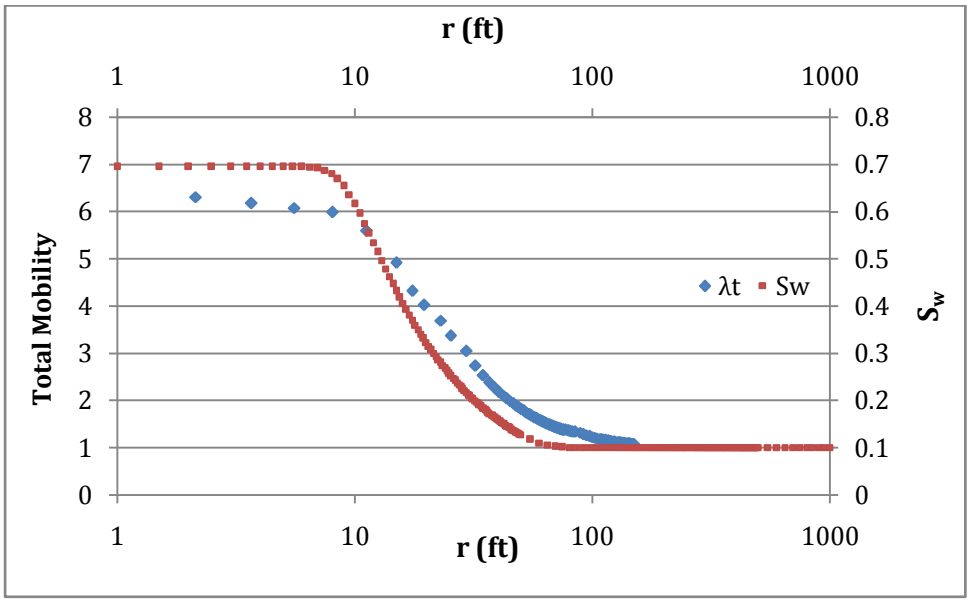

Figure 23: Total mobility and Water saturation vs radial distance

Reservoir mobility profile is also calculated by reading the saturation values at any given radial distance from the saturation profile at different time steps and then by using Eq 30 for $S_{wi} \leq S_w \leq (1\text{-}S_{or})$ from the relative permeability data, the total mobility is calculated. Figure 24 shows the comparison of the total mobility generated from the derivative curve λ_t and saturation curve λ_t (S_w). It is evident from Figure 24 that the total mobility estimated by two different approaches gives a close match. Table 8 Appendix A, shows the values and procedure involved to calculate the total mobility from the saturation curve.

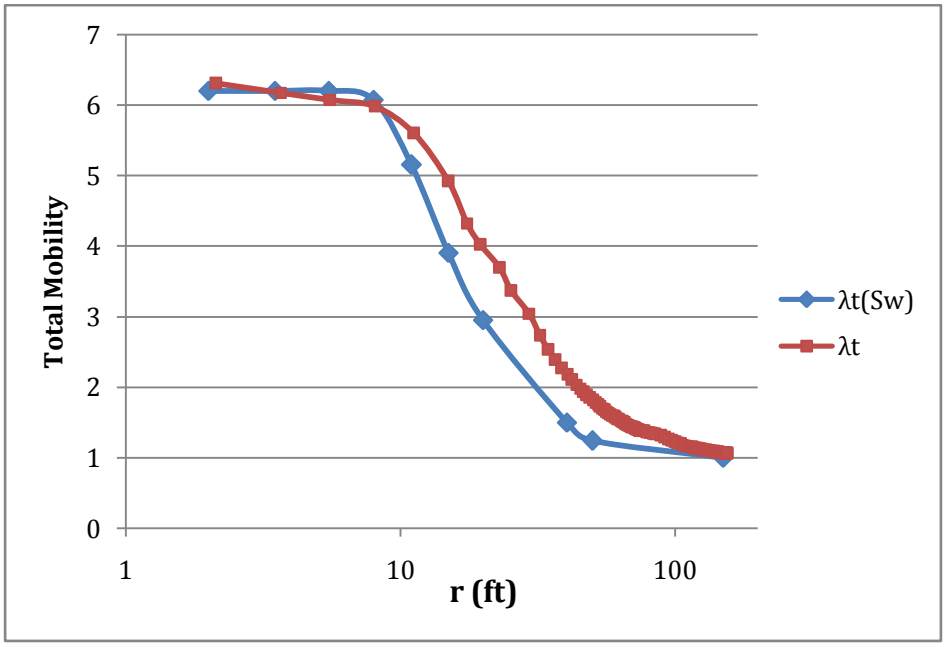

Figure 24: Comparison of Total mobility for derivative curve and saturation profile

4.3.5 Calculation of flood front radius

Distance to the leading edge of the injected fluid bank is calculated by the equations Eq (2.20) or Eq (2.21).

Using equation Eq (2.20) we first calculate the distance to the water bank and then compare it with the distance to the water bank obtained from equation Eq (2.21).

$$r_{f1} = \sqrt{\left[\frac{0.0002637\left(\frac{k}{\mu}\right)_1}{(\phi C_t)_1}\right]\left(\frac{\Delta t_{fx}}{\Delta t_{Dfx}}\right)}$$

Where

Δt_{fx} : Intersection time from the semi-log plot of shut-in time Δt vs. BHP

Δt_{Dfx} : Dimensionless intersection time obtained graphically from Figure 8

- Δt_{fx} is obtained by noting the intersection time from the Horner plot of Figure 18 and reading its corresponding value of shut-in time Δt = 5 hrs

- $\left(\frac{k}{\mu}\right)_1$ is the mobility of the flood out zone (water bank) from Figure 18 and was calculated to be 6.254
- $(\emptyset C_t)_1$ was obtained to be $1.41*10^{-6}$
- Δt_{Dfx} is obtained graphically using Figure 8 where $\frac{m_2}{m_1} = \frac{301.95}{52} = 5.806$ and specific storage ratio, $\frac{(\emptyset C_t)_1}{(\emptyset C_t)_2} = \frac{1.41*10^{-6}}{3.03*10^{-6}} = 0.465$, hence Δt_{Dfx} was found to be 4.25.

$$r_{f1} = \sqrt{\left[\frac{0.0002637 * 6.254}{1.41 * 10^{-6}}\right]\left(\frac{5}{4.25}\right)} = 37.1\ ft$$

Now using the material balance equation Eq (2.21)

$$r_{f1} = \sqrt{\frac{5.615 * q_w * t_{inj} * B_w}{\pi * \emptyset * h * \Delta S_w}} = \sqrt{\frac{5.615 * 200 * 10 * 1}{3.142 * 0.1 * 100 * 0.3}} = 34.51\ ft$$

From this we can conclude that the distance to the water bank is 34.5 ft away from the wellbore. The minor difference in both the results obtained could be due to the inaccurate estimation of Δt_{Dfx} graphically.

4.4 Effect of various parameters

Several parameters affecting the pressure response are considered to be studied, they include

- Viscosity of oil
- Skin effect
- Relative permeability
- Wellbore storage

4.4.1 Viscosity of Oil

Including the initial case with oil viscosity 10 cp i.e mobility ratio of 6.25, studies were carried out for oil viscosities of 2 and 0.8 cp having mobility ratios of 1.25 and 0.5 respectively. Water viscosity is the same as in the initial case, which is 0.4 cp. Mobility ratio of 0.5 @ μ_o 0.8 cp is a very favorable condition (M<1) where the displacement of oil by water occurs in a piston like manner. On the other hand, the mobility ratio of 6.25 @ μ_o 10 cp is considered as an unfavorable condition, (M>1) where water fingering occurs. Mobility ratio of 1.25 @ μ_o 2 cp is also considered as a favorable condition (M≅1, weak piston like displacement) where the mobility of the injected fluid (water) is the same as the reservoir oil.

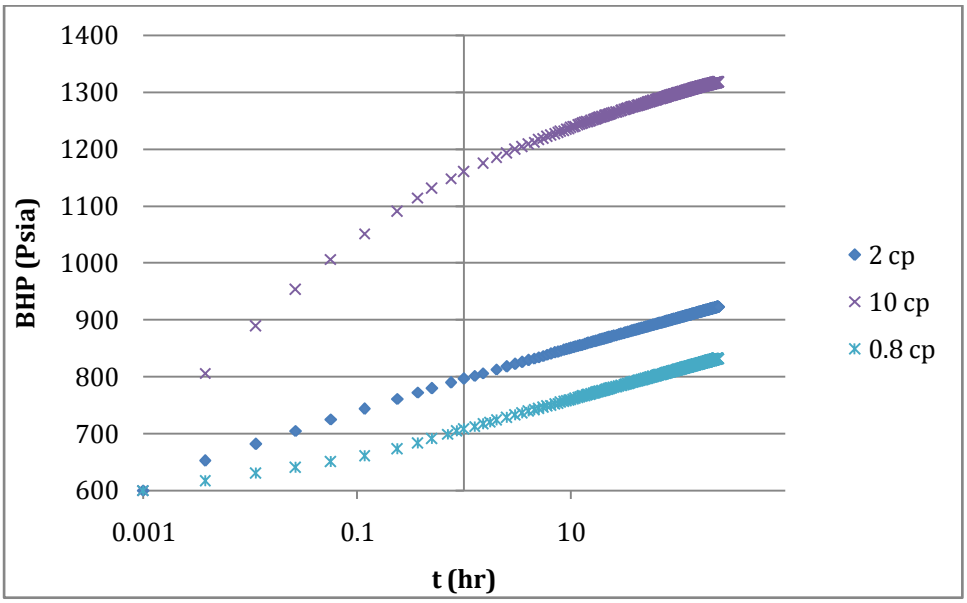

Figure 25: Injection pressure response, Bottom hole pressure vs. Injection time (hr) for μ_o of 10cp, 2cp and 0.8 cp

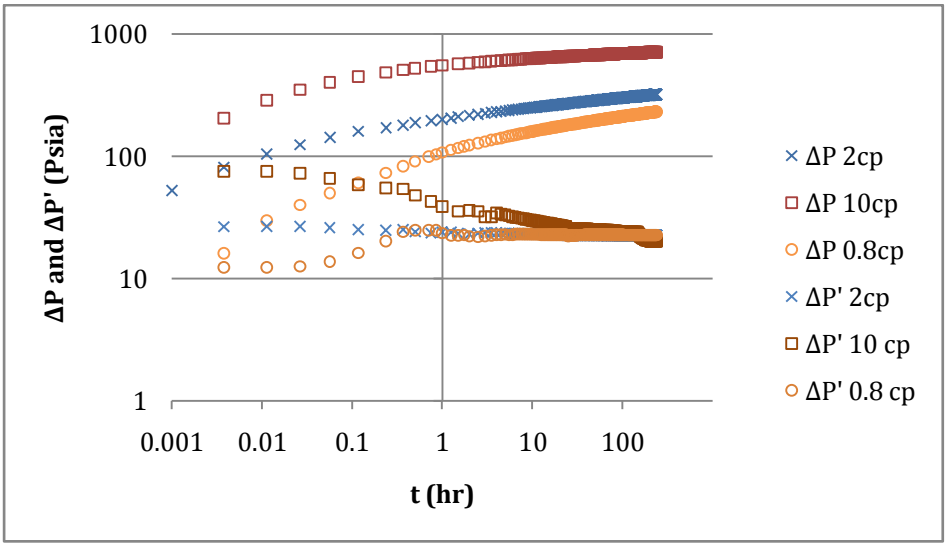

Figure 26: Injection pressure response, Pressure change and derivative vs. Injection time (hr) for μ_o of 10cp, 2cp and 0.8 cp

Figure 25 and Figure 26 shows the injection pressure response from the semi-log and log-log plot for 3 different mobility ratios respectively. From the cases where the viscosity of oil is 10 cp and 0.8 cp, 2 slopes are visible from the semi-log plot. This is due to an appreciable contrast of mobilities for the flooded and unflooded zones (water and oil banks). For the case where, the viscosity of oil is 2 cp with mobility ratio of almost 1, the semi-log plot shows a straight line indicating the mobilities of flooded and the unflooded zones (water and oil banks) are almost equal with a mobility ratio of 1.

Table 2: Comparison of calculated skin, and mobility from the injection pressure response, with the input values for μ_o of 10, 2 and 0.8 cp

	Skin		Mobility (cp)			
	Input	Calculation	Input		Calculation	
			Oil	Water	Oil	Water
10 cp	0	-0.04	1	6.25	1.8	6.57
2 cp	0	-0.238	5	6.25	5.27	6.25
0.8 cp	0	-0.17	12.5	6.25	11.47	6.13

Table 2 above compares the calculated skin and mobility with the input data for injection pressure response. In all the cases the mobility of the oil zone and the skin

estimated from the semi-log plot for injection analysis varied slightly when compared to the input values. Water mobility closely matched the input data.

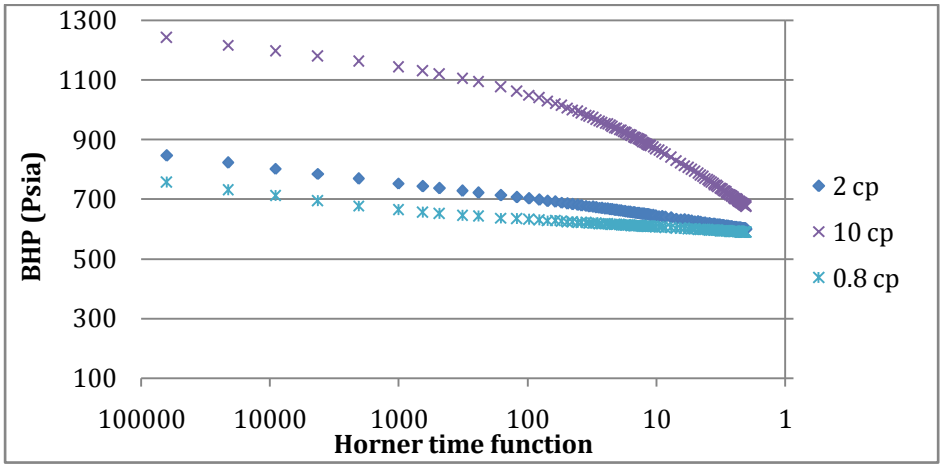

Figure 27: Falloff pressure response, Bottom hole pressure vs. Horner time function for μ_o of 10cp, 2cp and 0.8 cp

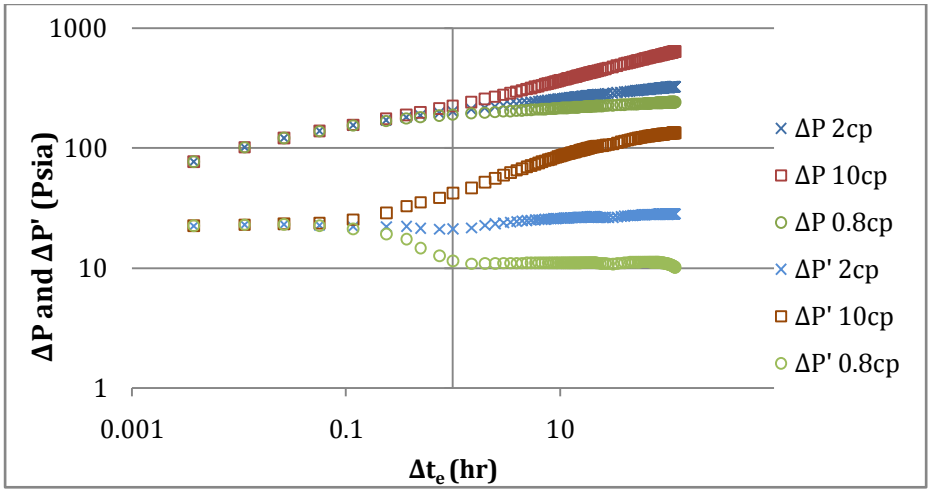

Figure 28: Falloff pressure response, Pressure change and derivative vs. falloff equivalent time for μ_o of 10cp, 2cp and 0.8 cp

Figure 27 and Figure 28 shows a semi-log and a log-log plot of falloff pressure response for three different oil viscosities. From the pressure change and derivative curves of log-log plot, two different zones can be easily identified ($\Delta t_e \leq 0.1$). All the curves overlap each other in the early time region until the flood out zone is reached and then separate at the start of the transition period.

Table 3: Comparison of calculated skin, and mobility from the falloff pressure response, with the input values for μ_o of 10, 2 and 0.8 cp

	Skin		Mobility (cp)			
	Input	Calculation	Input		Calculation	
			Oil	Water	Oil	Water
10 cp	0	0.019	1	6.25	1.07	6.253
2 cp	0	0.051	5	6.25	4.94	6.253
0.8 cp	0	-0.01	12.5	6.25	12.53	6.28

As compared to the injection results, falloff analysis gives more accurate results when calculated values of mobility and skin are compared with the input values, as shown in Table 3 above. This is because of the stationary banks of water and oil zones with almost no movement of fluids during falloff period. This ensures valid results to be obtained during the falloff tests. Figure 29 shows the total mobility profiles for three different viscosities of oil. Since the viscosity of water is unchanged for all the three cases the mobility profiles starts to deviate once the flood out zone is reached and finally approaches the unflooded zone mobility (oil bank mobility).

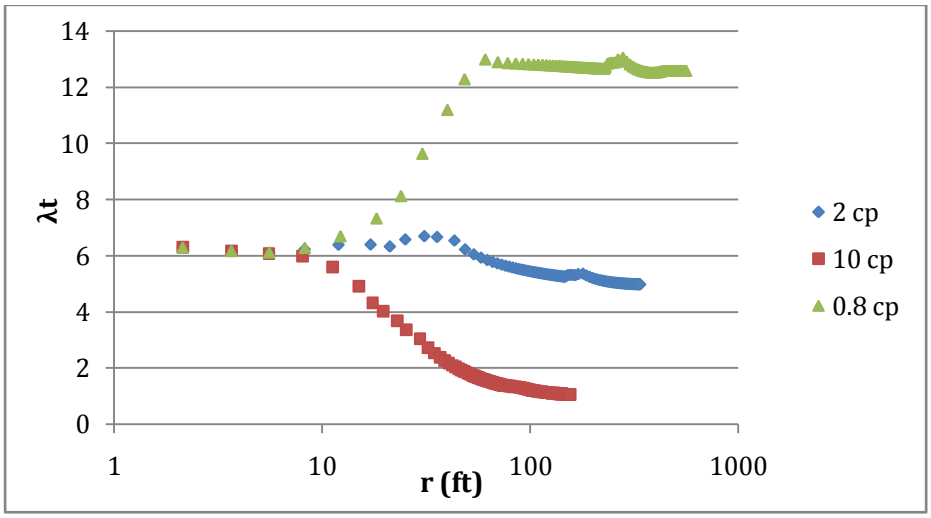

Figure 29: Total mobility vs. radial distance for μ_o of 10cp, 2cp and 0.8 cp

4.4.2 Skin effect

Effect of skin was studied for three cases, which include the initial case with zero skin and are compared with both positive and negative skin, -0.4 and +1.

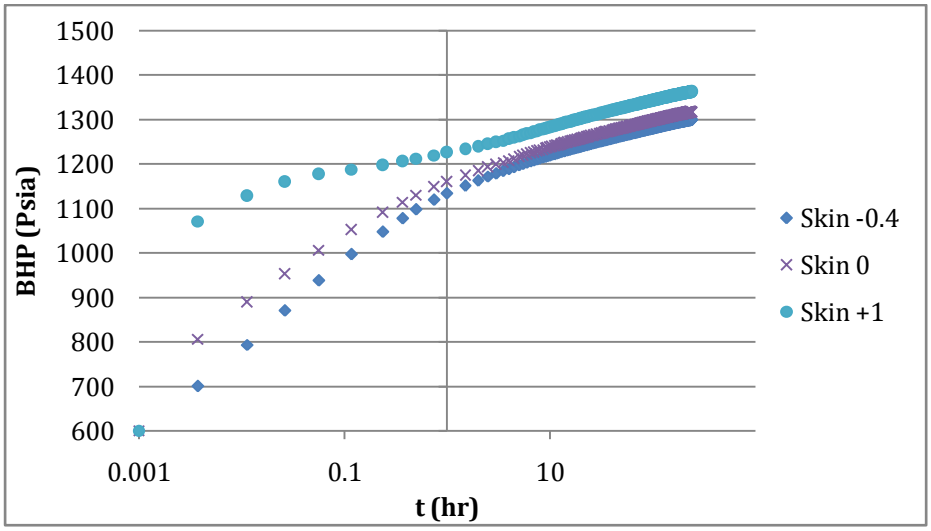

Figure 30: Injection pressure response, Bottom hole pressure vs. Injection time (hr) for 0, -0.4 and +1 skin factors.

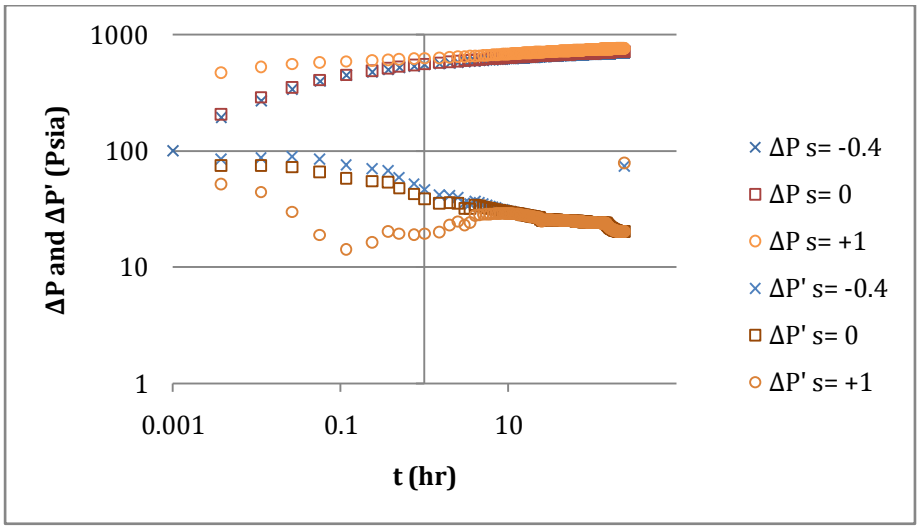

Figure 31: Injection pressure response, Pressure change and derivative vs. Injection time (hr) for 0, -0.4 and +1 skin factors

Figure 30 and Figure 31 shows a semi-log and a log-log plot for zero, positive and negative skins. It is clear from the injection plots that the skin factor has a certain impact in early time region, and then converging to a single curve when the skin effect is diminished as injection time increases.

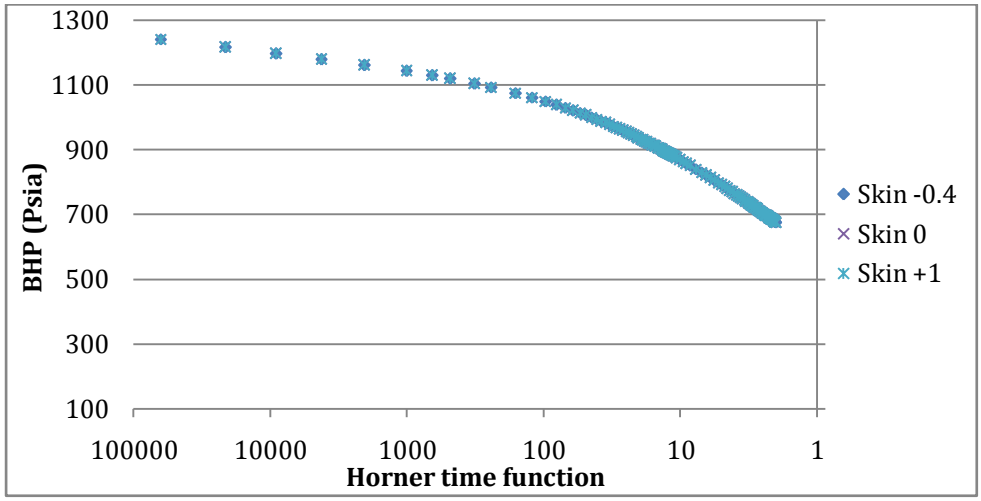

Figure 32: Falloff pressure response, Bottom hole pressure vs. Horner time function for 0, -0.4 and +1 skin factors

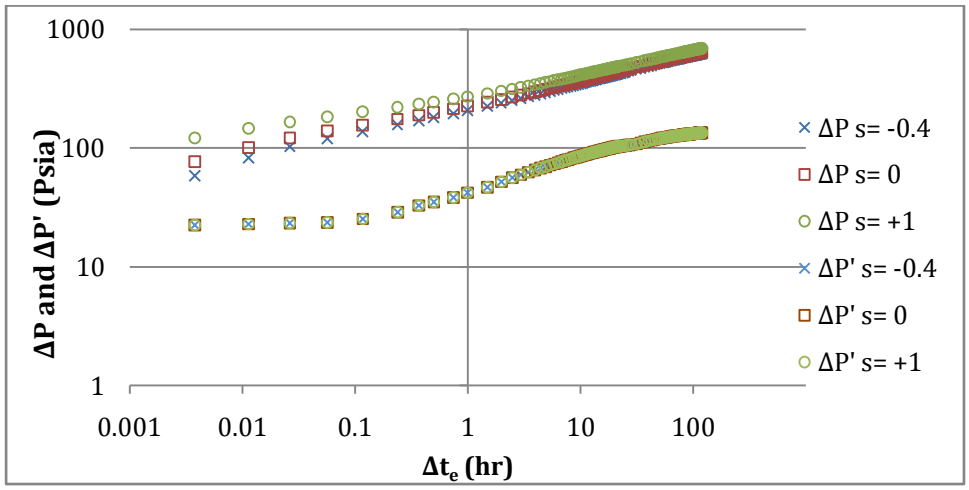

Figure 33: Falloff pressure response, Pressure change and derivative vs. falloff equivalent time for 0, -0.4 and +1 skin factors

With the absence of wellbore storage effect, it is known that skin has no effect on the pressure derivative and it just changes the pressure value by a factor S [**15**]. From the falloff curves we notice that the semi-log plot Figure 32 and derivative curve Figure 33 are identical for different skin factors and the pressure difference ΔP as a function of falloff equivalent time Δt_e are different for different skin effects. Although not shown here, Mobility profile and reservoir pressure profile were also found to be identical for different skin effects. Skin factor from the conventional semi-log analysis of the early time region is determined from the falloff tests and compared

with input skin values. The results are as shown in Table 4 where the evaluated skin matches very well with the input data.

Table 4: Comparison of calculated skin from the falloff pressure response, with the input values for skin of 0, -0.4 and +1

Skin	
Input	Calculation
0	0.019
-0.4	-0.388
+1.0	1.069

4.4.3 Relative Permeability

Different set of Relative permeability was used to study the pressure transient analysis. Relative permeability used is taken from [**18**]. Total mobility is calculated using equation Eq (4.4). Plot of relative permeability and total mobility chosen for this study is shown in Figure 34 and Table 9 Appendix A, shows the values used in the simulation model. Again an unfavorable mobility ratio of 4.921 was chosen for this case to distinguish the two zones easily.

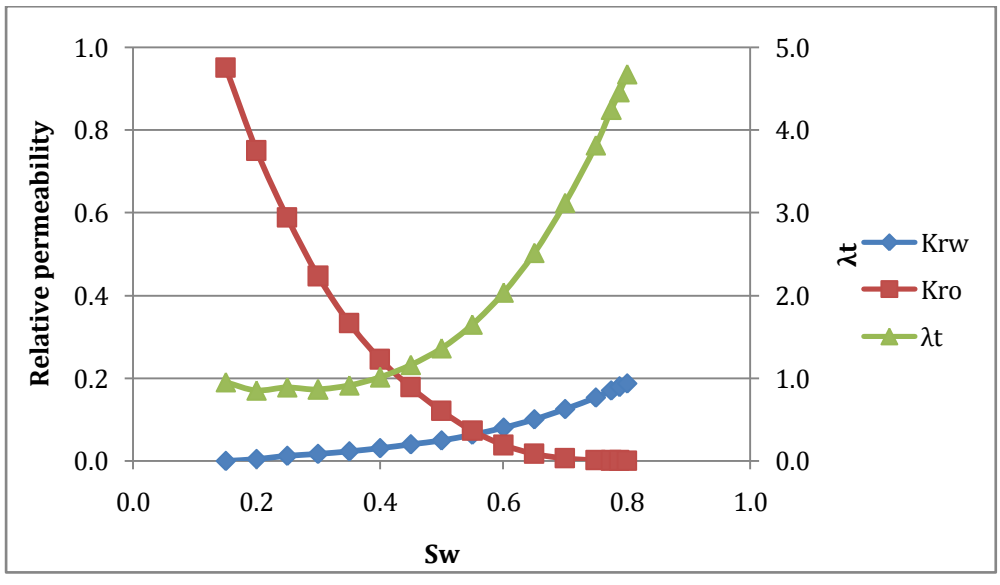

Figure 34: Relative permeability and Total mobility vs. Saturation (Set 2)

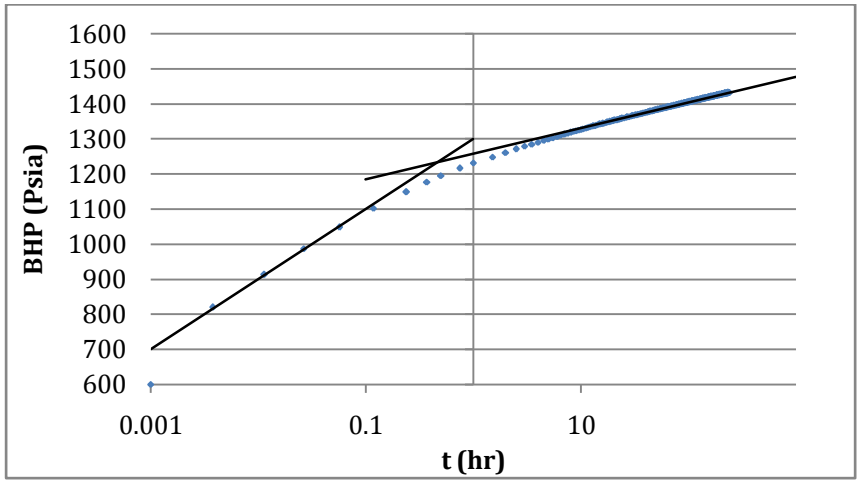

Figure 35: Injection pressure response, Bottom hole pressure vs. Injection time (hr) for Set 2 Relative permeability.

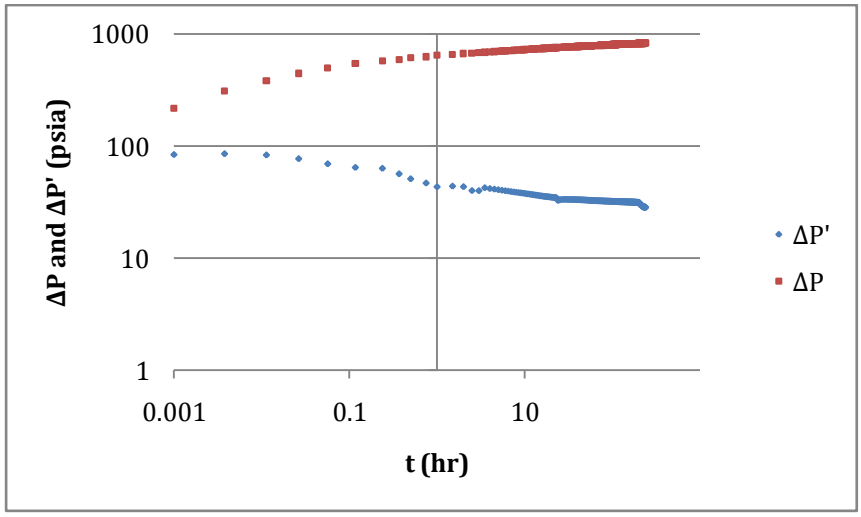

Figure 36: Injection pressure response, Pressure change and derivative vs. Injection time (hr) for Set 2 Relative permeability

Calculated skin factor obtained from the semi log plot from Figure 35 is 0.062 which is close to zero but the mobility of the oil zone showed considerable deviation from the input value which could be because of the moving banks as been discussed earlier. Whereas, from semi-log plot of falloff analysis Figure 37 gave a close match with the input data for the skin and mobility of oil and water banks.

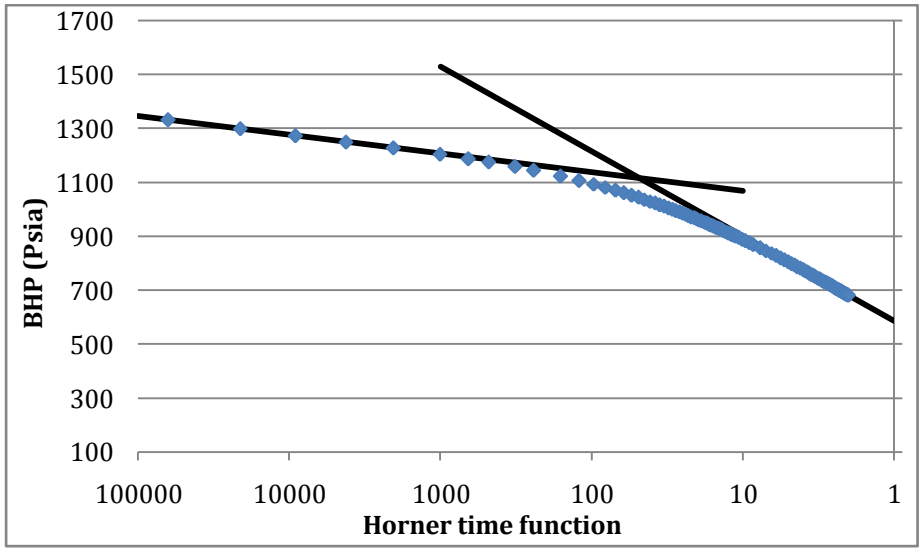

Figure 37: Falloff pressure response, Bottom hole pressure vs. Horner time function for Set 2 Relative permeability

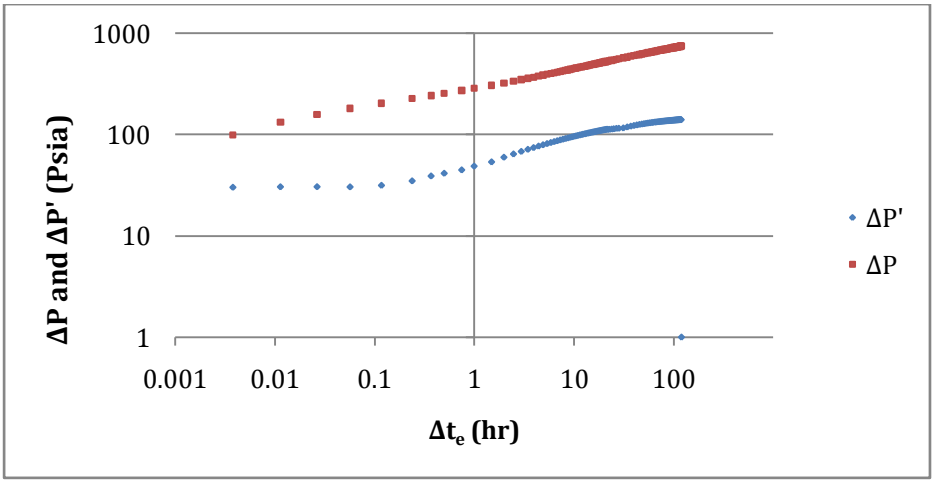

Figure 38: Falloff pressure response, Pressure change and derivative vs. falloff equivalent time for Set 2 Relative permeability

Distance to the leading edge of the injected fluid bank r_{f1} was estimated to be 32 ft using equation Eq (2.20) and Eq (2.21). Total mobility profile from the derivative curve is generated using the equations Eq (2.22) and Eq (2.23) representing the flood out zone (water bank) and the unflooded zone (oil bank). From Figure 39 it is clearly observed that, the total mobility profile follows the curve of water saturation profile generated from ECLPISE at the end of falloff period (20 days). This shows that multibank analysis method can also be applied for different set of relative permeability curves.

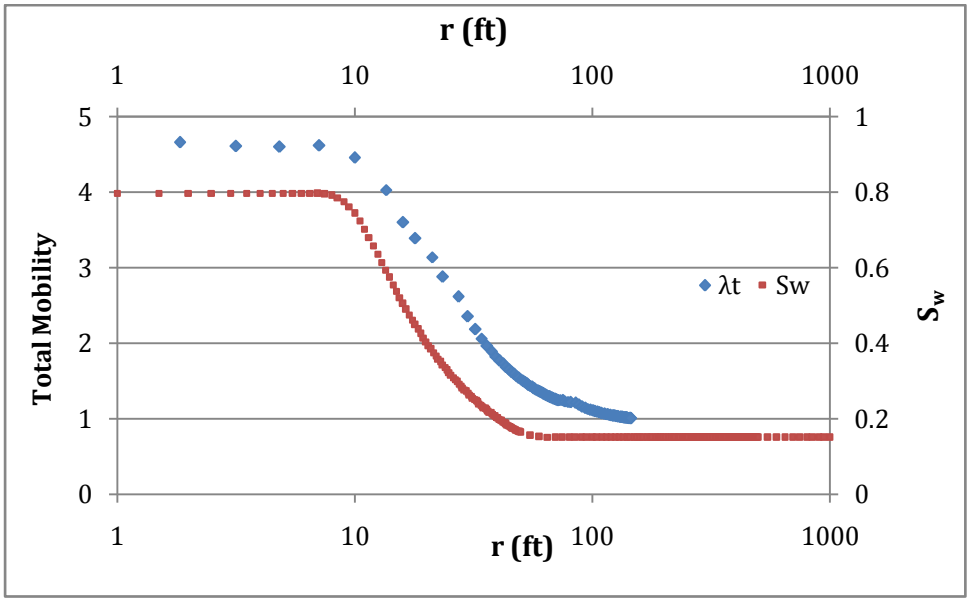

Figure 39: Total mobility and Water saturation vs radial distance for Set 2 Relative permeability

4.4.4 Wellbore Storage

When a well is opened to flow or shut in, the rate change at the surface is not instantaneously transmitted to the sand face. The actual rate at which the change is transmitted to the sand face is a function of the distance to the sand face and the compressibility of the medium through which it travels. As a result, there is a gradual change in rate to the desired value. This phenomenon is called wellbore storage. Effect of wellbore storage is studied here which includes the initial case with zero wellbore storage and is compared when CD = 500.

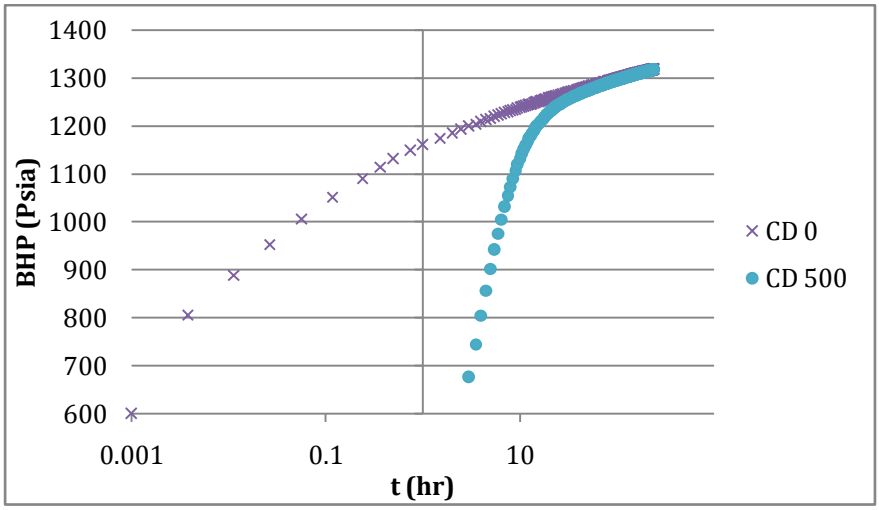

Figure 40: Injection pressure response, Bottom hole pressure vs. Injection time (hr) for CD = 0 and 500.

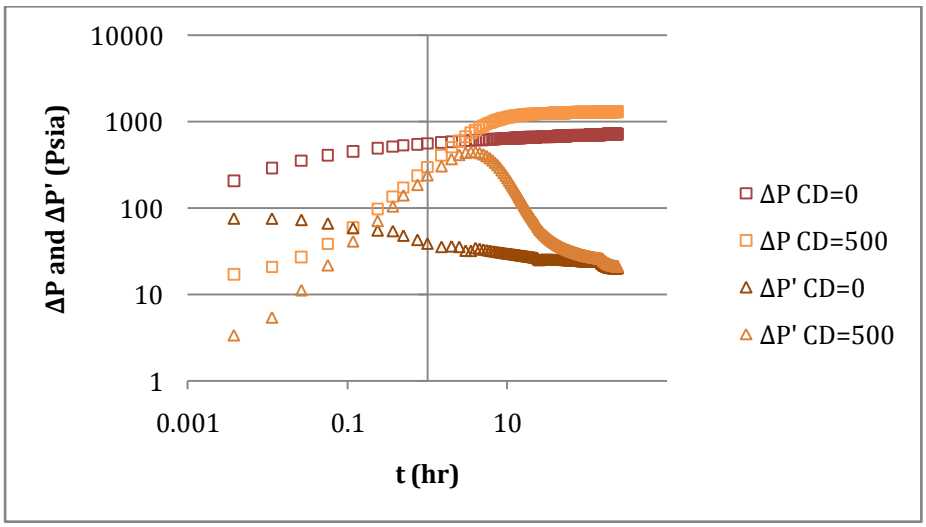

Figure 41: Injection pressure response, Pressure change and derivative vs. Injection time (hr) for CD = 0 and 500.

Wellbore storage effects are dominant during the early time region. During this period the pressure difference ΔP and derivative ΔP' produce a 45^{o} straight line on the log-log plot and a 'hump' is observed on the derivative curve during the transition from early time region (where wellbore storage effect is dominant) to the infinite acting radial flow system, as shown in Figure 41. From the plot of the derivative curve we can estimate the end of wellbore storage effect, which is around 40 hrs since the start of injection.

From Figure 42 and Figure 43 for falloff pressure response we see the deviation in the early time region due to presence of wellbore storage effect and the curves finally merge when the effect of wellbore storage reduces to zero. Normally the early time pressure data are misinterpreted due to the wellbore storage effects. Elimination of this skewed data points is very important to accurately interpret early time region, which is extremely important in pressure transient analysis. The saturation profiles with and without wellbore storage was found to be identical but the mobility profile was distorted until the end of early time region as mobility profile is generated using the derivative curve.

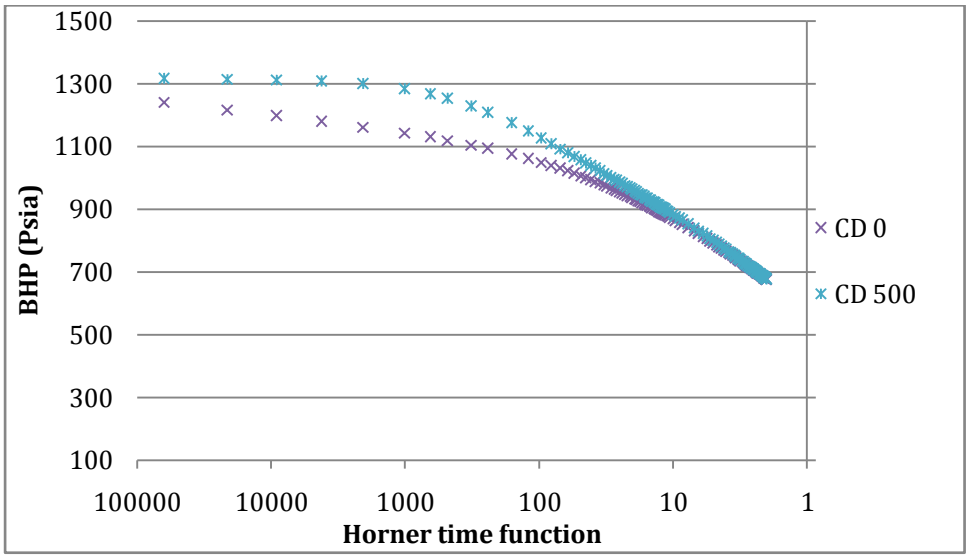

Figure 42: Falloff pressure response, Bottom hole pressure vs. Horner time function for CD = 0 and 500.

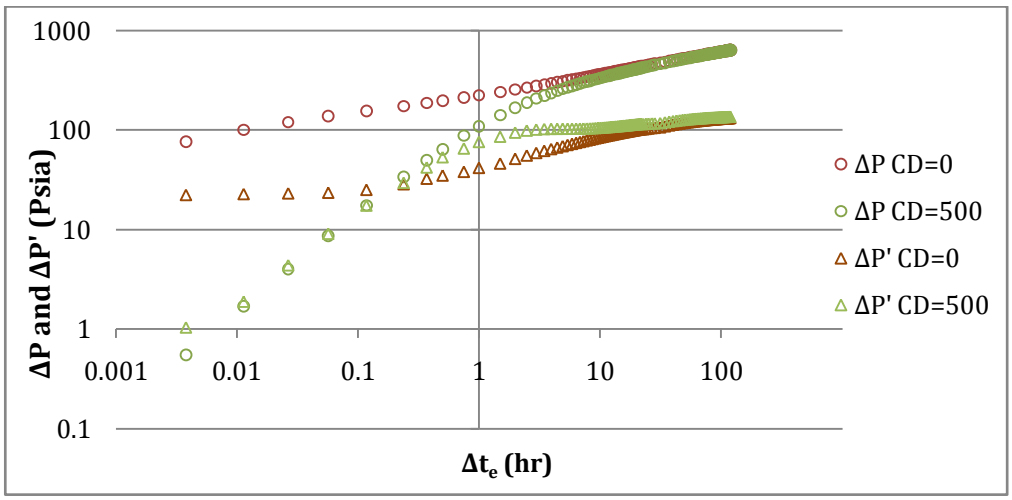

Figure 43: Falloff pressure response, Pressure change and derivative vs. falloff equivalent time for CD = 0 and 500.

CHAPTER 5

CONCLUSIONS AND RECOMENDATIONS

5.1 Conclusions

Pressure transient analysis of injection wells has been studied extensively for water-oil system by creating a reservoir model using numerical simulation. From the results obtained, the following conclusions can be made:

1. Falloff pressure analysis is more accurate than injection pressure analysis for the estimation of skin, permeability and mobilities for flooded and unflooded zones due to the stationary fluid banks.

2. Total mobility profiles generated from the derivative curve and saturation curve are almost identical.

3. The two methods (material balance and Merill [**12**]) used to determine the distance to the leading edge of the injected fluid bank, gave almost the same results.

4. The multibank analysis method for pressure transient analysis is applicable to different relative permeability curves and as well as to different mobility ratios.

5. The presence of skin factor when compared to zero skin, has no effect on the derivative curve $\Delta P'$, saturation profile and the total mobility profile. Only the pressure difference ΔP as a function Δt are different for different skin effects.

6. It is important to eliminate the effect of wellbore storage in order to accurately interpret the early time pressure data, which is extremely important to the pressure transient analysis.

5.2 Recommendations

Well testing is a vast field where a huge amount of research has already been done and also many new ideas to improve the accuracy of pressure transient analysis for various systems are in-progress. For future research to advance the analysis carried out in this thesis, following recommendations are made:

- Wellbore storage effects needs to be minimized or eliminated for accurate interpretation of the early time region which was not considered in this thesis.

- Effect on pressure behavior, as in a real field caused by, reservoir boundaries or barriers, compressibility, presence of a strong aquifer for pressure support, disturbance caused by nearby injection or production wells, can also be considered.

- Reservoir heterogeneity, like presence of permeability barriers, fractures, faults etc, needs to be considered which gives a feel of real field data interpretations.

- Pressure transient analysis for different injection fluids could be carried out, like gas injection, steam injection etc.

- Considerations of pressure transient analysis through multiple fluid banks could be important when water alternating gas (WAG) injection is carried out.

REFERENCES

[1] *Reservoir Engineering*. Edinburgh, Scotland: Heriot Watt Institute of Petroleum Engineering, 2005.

[2] *Well Test Analysis*. Edinburgh, Scotland: Heriot Watt Institute of Petroleum Engineering, 2005.

[3] John Lee , John B. Rollins , and John P. Spivey , *Pressure Transient Testing*. Texas A&M U: Society of Petroleum Engineers Inc., vol. 9.

[4] Ahmed Tarek and D. Nathan Meehan, *Advanced Reservoir Management and Engineering*, 2nd ed., 2012.

[5] Tarek Ahmed, *Reservoir Engineering Handbook*, 2nd ed. Houston, Texas: Gulf Publishing Company , 2001.

[6] P. Hazebroek and C.S. Matthews, "Pressure Falloff in Water Injection Wells," *Transaction, AIME*, 1958.

[7] N.S. Yeh and R.G. Agarwal, "Pressure Transient Analysis of Injection Wells in Reservoirs With Multiple Fluid Banks," in *SPE Annual Technical Conference and Exhibition*, San Antonio, Texas, 1989.

[8] Anil Kumar Ambastha, "Pressure Transient Analysis for Composite Systems," Stanford, California, PhD Thesis 1988.

[9] S.E. Buckley and M.C. Leverett, "Mechanism of Fluid Displacement in Sands," *Transaction of the AIME*, 1942.

[10] M.C. Leverett, "Capillary Behavior in Porous Solids," *Transactions of the AIME*, 1941.

[11] M.A. Sabet, *Well Test Analysis*. Houston, Texas: Gulf Publishing Company, 1991, vol. 8.

[12] L.S. Merrill, Hossein Kazemi, and W. Barney Gogarty, "Pressure Falloff Analysis in Reservoirs With Fluid Banks," *Journal of Petroleum Technology*, 1974.

[13] Hossein Kazemi, L.S. Merrill, and J.R. Jargon, "Problems in Interpretation of Pressure Fall-Off Tests in Reservoirs With and Without Fluid Banks," *Journal of*

Petroleum Technology, 1972.

[14] A. Sosa, R. Raghavan, and T.J. Limon, "Effect of Relative Permeability and Mobility Ratio on Pressure Falloff Behavior," *Journal of Petroleum Technology*, 1981.

[15] Noaman A.F. El-Khatib, "Transient Pressure Behaviour of Composite Reservoirs With Moving Boundaries," in *Middle East Oil Show and Conference*, Bahrain, 1999.

[16] Michael M. Levitan, "Application of Water Injection/Falloff Tests for Reservoir Apprisal: New Analytical Solution Method for Two-Phase Variable Rate Problem," *SPE 77532*, 2002.

[17] Amina A. Boughrara, Alvaro M.M. Peres, Shi Chen, Augusto A. V. Machado, and Albert C. Reynolds, "Approximate Analytical Solutions for the Pressure Response at a Water-Injection Well," *SPE 90079*, 2006.

[18] Weiping Yang and R.A. Wattenbarger, "Water Coning Calculations for Vertical and Horizontal Wells," *SPE 22931*, 1991.

[19] Charles R. Smith, G.W. Tracy, and L. Lance Farrar, *Applied Reservoir Engineering*. Oklahoma: Oil and Gas Consultants International, Inc., 1999, vol. 2.

[20] Amanat U. Chaudhry, *Oil Well Testing Handbook*. Houston, Texas: Advanced TWPSOM Petroleum Systems, Inc., 2004.

[21] Roland N. Horne, *Modern Well Test Analysis*, 2nd ed. California: Petroway, Inc., 1995.

APPENDIX A

Table 5: Relative permeability and total mobility values

S_w	K_{ro}	K_{rw}	λ_t
0.1000	1.0000	0.0000	1.0000
0.2000	0.4823	0.0002	0.4871
0.3000	0.1975	0.0031	0.2747
0.4000	0.0625	0.0156	0.4531
0.5000	0.0123	0.0494	1.2469
0.6000	0.0008	0.1206	3.0149
0.7000	0.0000	0.2500	6.2500

λ_w	λ_o	M
6.25	1	6.25

Table 6: Calculation of derivative values

Time	WBHP	Pressure			
hr	Psia	change	Lnt	slope	ΔP'
0	600				
0.0038	805.93896	205.94	-5.5787	75.499	75.499
0.0113	888.88281	288.88	-4.4800	75.298	75.398
0.0264	952.68256	352.68	-3.6327	70.256	72.777
0.0567	1006.2271	406.23	-2.8706	62.197	66.226
0.1171	1051.3785	451.38	-2.1447	54.762	58.480
0.2380	1090.2126	490.21	-1.4355	55.267	55.014
0.3690	1114.45	514.45	-0.9970	52.911	54.089
0.5000	1130.5255	530.53	-0.6931	42.883	47.897
0.7500	1147.9131	547.91	-0.2877	42.685	42.784
1.0000	1160.1929	560.19	0.0000	34.846	38.766
1.5000	1174.3218	574.32	0.4055	36.143	35.495

2.0000	**1184.7196**	**584.72***	**0.6931***	**35.850***	**35.996***
2.5000	1192.7192	592.72	0.9163	35.092	35.471

Pressure Change = 1184.72 – 600 = 584.72

Lnt = Ln(2) = 0.6931

Slope = (592.72 – 584.72) / (0.9163- 0.6931) = 35.85

ΔP' = (36.143 + 35.850) / 2 = 35.996

Table 7: Total mobility from derivative curve

Δt_e	ΔP'	λ_t	r
0.00378	22.39914	6.3056	2.139224
0.011329	22.86909	6.176021	3.665302
0.026437	23.25071	6.074652	5.552878
0.056667	23.61232	5.981622	8.067217
0.117063	25.23445	5.597111	11.21611
0.237764	28.73523	4.915221	14.97943
0.368444	32.67661	4.322358	17.48624
0.49896	35.14539	4.018735	19.62133
0.747664	38.28262	3.689402	23.01345
0.995861	41.95032	3.36684	25.37237
1.490683	46.39618	3.044216	29.5176
1.983471	51.7332	2.730162	32.24466
2.474237	**55.86073**	**2.528431***	**34.65746***
2.962963	59.2843	2.382418	36.81482

$$\lambda_t = \frac{70.6qB}{h\Delta P'_{wf}} = \frac{70.6 * 200 * 1}{100 * 55.861} = 2.528$$

$$r = 0.024\left[\frac{\lambda_t \Delta t_e}{\emptyset c_t}\right]^{0.5} = 0.024 * \left[\frac{2.528 * 2.4742}{0.1 * (3 * 10^{-5})}\right]^{0.5} = 34.657$$

Table 8: Total mobility from saturation profile

Δt	r	S_w	K_{rw}	K_{ro}	$\lambda_{t(Sw)}$
0.00378	2	0.694628	0.247762	0.008953	6.202997
0.01133	3.5	0.69468	0.247783	0.008867	6.203447
0.02644	5.5	0.694653	0.247772	0.008911	6.203216
0.05668	8	0.68003	0.241679	0.033283	6.075267
0.11712	11	0.574505	0.19771	0.209158	5.151919
0.238	15	0.431801	0.13825	0.446998	3.90326
0.5	20	0.322735	0.092806	0.628775	2.948932
4.00001	40.5	0.15704	0.023767	0.904933	1.4991
7.5	50	0.127414	0.011423	0.954309	1.239877
203.9999	150	0.1	0	1	1

1. Δt and its corresponding r obtained from the total mobility generated from the derivative curve is noted at any given point.
2. S_w is read from the saturation profile at the same Δt (time step) and r that were noted from step 1.
3. k_{ro} and k_{rw} are estimated from the relative permeability curves at the corresponding S_w from step 2.
4. $\lambda_{t(Sw)}$ is then calculated using equation Eq (4.4).

Table 9: Relative permeability and total mobility (Set 2)

Sw	Krw	Kro	λt
0.1500	0.0000	0.9500	0.9500
0.2000	0.0040	0.7500	0.8500
0.2500	0.0120	0.5876	0.8876
0.3000	0.0166	0.4462	0.8612
0.3500	0.0232	0.3325	0.9125
0.4000	0.0305	0.2450	1.0075
0.4500	0.0392	0.1770	1.1570
0.5000	0.0497	0.1200	1.3625

0.5500	0.0630	0.0724	1.6474
0.6000	0.0798	0.0374	2.0324
0.6500	0.1000	0.0163	2.5163
0.7000	0.1244	0.0056	3.1156
0.7500	0.1525	0.0008	3.8133
0.7750	0.1698	0.0004	4.2454
0.788	0.1784	0.0002	4.4602
0.8	0.1870	0.0000	4.6750

λw	λo	M
4.675	0.95	4.921

APPENDIX B

Eclipse 100 data file:

```
============================================================
RUNSPEC

TITLE
Pressure transient analysis in Injection Wells

DIMENS
  210       1          1 /

OIL
WATER

RADIAL

FIELD

NSTACK
20/

WELLDIMS
5         1         5         5 /

TABDIMS
1/

START
01 JAN 2012/

UNIFOUT
```

```
============================================================
GRID

INRAD
0.5 /

--
DRV
100*0.5 90*5 20*50 /

OUTRAD
1500 /

DTHETAV
360 /


EQUALS
-- Keyword value X1 X2 Y1 Y2 Z1 Z2

DZ          100   1   210   1   1   1   1 /
TOPS        1500  1   210   1   1   1   1 /
PERMR       10    1   210   1   1   1   1 /
PORO        0.1   1   210   1   1   1   1 /
/

COPY
PERMR PERMTHT /
PERMR PERMZ /
/
INIT
============================================================
PROPS
```

GRAVITY

1* 1 /

PVCDO

600 1 3E-05 10

/

PVTW

600 1* 3E-06 0.4 0.0/

ROCK

600 3.00E-06 /

SWOF

0.15	0	0.95	0
0.2	0.004	0.75	0
0.25	0.012	0.5876	0
0.3	0.0166	0.4462	0
0.35	0.0232	0.3325	0
0.4	0.0305	0.245	0
0.45	0.0392	0.177	0
0.5	0.0497	0.12	0
0.55	0.063	0.0724	0
0.6	0.0798	0.0374	0
0.65	0.1	0.0163	0
0.7	0.1244	0.0056	0
0.75	0.1525	0.0008	0
0.775	0.1698	0.0004	0
0.788	0.1784	0.0002	0
0.8	0.187	0	0

/

==========

REGIONS

```
EQUALS

SATNUM      1        1        210     1        1        1        1 /
/
============================================================
SOLUTION

EQUIL
1550    600      1600    0/

RPTRST

BASIC=2 NORST=1/
============================================================
SUMMARY

FPR

WBHP
/

FOPR

FWIR

FWIT

FWPR

FOPT

FWPT
```

```
WBHP
/
WWCT

PROD/

TCPU

EXCEL
============================================================
SCHEDULE

RPTRST

BASIC=2 NORST=1/

TUNING
--TSINIT TSMAXZ TSMINZ TSMCHP TSFMAX TSFMIN TSFCNV TFDIFF
0.000157401     1     0.000015740     1     0.000058657     2     0.3    0.1    1.25 /
/
/



WELSPECS
INJ     G1      1       1       1500    WATER/
/

COMPDAT

INJ     1       1       1       1       OPEN          2*       1 /
/

WCONINJ
INJ     WAT           OPEN          RATE          200             3*       4000/
```

/

TSTEP
48*0.0208333 216*0.041666666 /

INCLUDE
'include-files\Falloff-after-100days.INC' /

END